weakness of CTL response. Therefore, for the establishment of the effective therapy of type B CH, it is necessary to elucidate the reason for the weakness of CTL response and to seek the method for boosting the response.

In addition, the mechanism for the development of CH from ASC state still remains unknown. Breaking tolerance in a CTL level should be one of the key mechanisms for this phenomenon. To confirm the hypothesis above and to establish therapeutic model, an appropriate animal model system is necessary because of the technical and ethical difficulties in human study.

Studies on HBV have progressed rapidly since the HBV transgenic mice system was established by Chisari *et al.* (5). With this system, it has been has proven that HBV-specific CTLs cause acute or fulminant hepatitis (6) and are directly cytopathic *in vivo* (7). In addition, with this system, it has been shown that HBV-specific CTLs have mechanism to suppress HBV gene expression and replication without killing hepatocytes (8, 9), although the destruction of both infected and bystander cells by CTLs are thought to be another important mechanism to terminate viral infection (10, 11). Since HBV transgenic mice used in our study is deeply tolerant against HBsAg in both cellular and humoral immune responses, it may be a suitable model to study the mechanism for breaking tolerance and the immunological treatment for chronic HBV infection.

Recently, a novel lymphoid lineage, $V\alpha14^+$ NKT cells, distinct from mainstream T cells, B cells and NK cells has been identified (12, 13). These cells are found in relative abundance in tissue such as spleen, bone marrow, thymus and liver and characterized by the co-expression of NK cell receptors and semi-invariant T cell receptors encoded by Vα14 and Jα18 gene segments. It is well known that activated $V\alpha14^+$ NKT cells strongly produce $T_h1$ and two cytokines, and we expected that this cell fraction can affect CTL induction.

We here report that NKT cell activation strongly helps to induce specific CTLs by the HBsAg immunization even in HBV transgenic mice, deeply tolerant to HBsAg in a CTL level. We think that our findings may help explaining the development of CH from ASC state and that they may suggest the novel immunological approach for the treatment of CH B.

## Methods

### *Mice*

Male BALB/c ($H\text{-}2^d$) and B10.D2 ($H\text{-}2^d$) mice (8–10 weeks, 25–30 g) were obtained from Japan SLC Inc. (Shizuoka, Japan). HBsAg transgenic mice lineage 107-5D [official designation Tg (Alb-1, HBV) Bri66; inbred B10.D2, $H\text{-}2^d$] in which the HBV envelope-coding region is under the control of the mouse albumin promoter was generously provided by Francis V. Chisari (Department of Molecular and Experimental Medicine, Scripps Research Institute, La Jolla, CA, USA). Mice deficient in Vα14 NKT cells [Jα281 knockout (KO)] were established by specifically deleting the Jα18 gene segment by homologous recombination (14) and backcrossed with BALB/c mice.

### *Cell lines and reagents*

The $H\text{-}2^d$ mastcytoma cell line P815 was obtained from the American Type Culture Collection (Rockville, MD, USA). P815 cells expressing HBV-preS1, 2 and S (P815preS1) and the HBsAg-specific $CD8^+$ CTL clone 6C2 were generously provided by Francis V. Chisari (6, 7). mAbs specific to murine IL-2 (clone JES6-1A12), IL-4 (clone 30340.11), IFN-γ (clone H22), tumor necrosis factor (TNF)-α (TN3-19.12) and CD40L (clone 208109) were purchased from R&D Systems (Minneapolis, MN, USA). Recombinant murine IL-2 and CD40L were purchased from R&D Systems. PE-conjugated anti-mouse CD40L (clone MR1) was purchased from eBioscience.

### *Establishment of HBsAg-specific CTLs*

Immunization was performed using HBsAg (Advanced ImmunoChemical Inc., Long Beach, CA, USA) with or without alpha-galactosylceramide (α-GalCer) (generously provided by the Pharmaceutical Research Laboratory, Kirin Brewery, Gunma, Japan). HBsAg was intra-peritoneally (i.p.) administered at a dose of 10 μg per mouse in 0.2 ml of PBS (Invitrogen Corp. Carlsbad, CA, USA). α-GalCer was administered i.p. at a dose of 1 μg per mouse in 0.2 ml of PBS. In some experiments, IL-2 ($4 \times 10^4$ U per mouse) and/or CD40L (100 μg per mouse) were administered i.p. instead of α-GalCer. Spleen cells were prepared from immunized mice 7 days after the immunization. The immunized spleen cells ($4 \times 10^6$ per well) were cultured in 24-well plates with mitomycin C (MMC)-treated P815preS1 ($2 \times 10^5$ per well) in complete RPMI 1640 (Sigma–Aldrich, St Louis, MO, USA) containing 10% heat-inactivated FCS (Invitrogen Corp.) and 5% EL-4 supernatant as a source of T cell growth factor. The immunized spleen cell lines and clones were re-stimulated with MMC-treated spleen cells ($4 \times 10^6$ per well) and P815preS1 ($2 \times 10^5$ per well) every 7 days. HBsAg-specific CTL clones were established by limiting dilution.

### *Blocking experiment using neutralizing antibodies to IL-2, IL-4, IFN-γ, TNF-α and CD40L*

To evaluate the role of various cytokines and ligands in the induction of HBsAg-specific CTLs *in vivo*, mAbs to IL-2, IL-4, IFN-γ, TNF-α and CD40L (100 μg per mouse) were administered i.p. on days 0 and 3 of the immunization with HBsAg or HBsAg and α-GalCer. After re-stimulation *in vitro*, the proportion of HBsAg-specific cells was measured by flow cytometric analysis using a FACScan (Becton Dickinson Immunocytometry Systems, San Jose, CA, USA). The mAbs to IL-2, IL-4, IFN-γ, TNF-α and CD40L were purchased from R&D Systems.

### *Cytotoxicity assay*

The cytolytic activity of HBsAg-specific CTLs was assessed using a Europium release assay as described previously (15). Target cells (P815 or P815preS1) were labeled with Eu diethylenetriaminepentaacetate (80 mM; Wako Pure Chemical Industries Ltd, Osaka, Japan). Labeled targets ($5 \times 10^3$ cells) and various number of effector cells were added in a final volume of 200 μl to each well of 96-well round-bottomed

plates and incubated for 4 h at 37°C. Next, 20 μl of the culture supernatant was mixed with 100 μl of enhancing solution (Wallac Oy, Tuerku, Finland), and the released Eu was measured using a time-resolved fluorometer (1230 Arcus, Wallac Oy). The percentage of Eu release was determined from the following equation: %Eu release = [(experimental release − spontaneous release)/(maximal release − spontaneous release)] × 100. Maximal release was measured after lysis with Triton X-100. Spontaneous release was 10–20% of maximal release.

*Detection of HBsAg-specific CTLs by flowcytometry*

Immunodominant HBsAg-specific CTLs in mice are known to be restricted by H-2L$^d$ of MHC class I, and the shortest peptide HBsAg peptide resulting in maximal activity is S28–39 (IPQSLDSWWTSL) (HBsAgS28–39) (7). Therefore, peptide-loaded recombinant soluble dimeric mouse H-2L$^d$:Ig (mouse IgG1; BD PharMingen, San Diego, CA, USA) was prepared by mixing soluble dimeric mouse H-2L$^d$:Ig for 48 h at 4°C with a 160-fold molar excess of HBsAgS28–39. The peptide-loaded soluble dimeric mouse H-2L$^d$:Ig (4 μg) was then added to CD8$^+$ cells prepared from immunized splenocytes or re-stimulated splenocytes. After incubation for 1 h at 4°C, the cells were stained with FITC-conjugated anti-mouse CD8α and PE-conjugated anti-mouse IgG1 (BD PharMingen). The proportion of HBsAg-specific cells was measured by flow cytometric analysis on a FACScan (Becton Dickinson Immunocytometry Systems).

*Frequency analysis for HBsAg-specific CTLs by limiting dilution*

We performed limiting dilution analysis as previously described (16). CD8-positive cells from the immunized mice were isolated by using MACS system. These CD8-positive cells (three cells per well) were cultured in 96-well plates with MMC-treated spleen cells ($4 \times 10^5$ per well) and MMC-treated P815preS1 ($2 \times 10^4$ per well) in complete RPMI 1640 and 5% EL-4 supernatant. The cells were re-stimulated with MMC-treated spleen cells and P815preS1 every 7 days. After 14 days, the number of wells in which the cells proliferated was counted and the proportion of HBsAg-specific CTLs was measured by flow cytometric analysis on a FACScan as described above.

*Isolation of Vα14$^+$ NKT, CD4$^+$ T and CD8$^+$ T cells*

Spleen cells were separated into NK marker-positive and -negative cells using anti-DX5-conjugated magnetic beads (Miltenyi Biotec GmbH, Bergisch Gladbach, Germany). To label Vα14$^+$ NKT cells with recombinant soluble dimeric mouse CD1d:Ig (BD PharMingen), DX5-positive cells were mixed with recombinant soluble dimeric mouse CD1d:Ig that had been pre-incubated with a 40-fold molar excess of the Vα14$^+$ NKT cell-specific ligand α-GalCer. After thorough washing, the stained cells were incubated with rat anti-mouse IgG1-conjugated immunomagnetic beads (Dynal Biotech ASA, Oslo, Norway). Bead-bound cells were magnetically removed using magnetic particle concentrator-1 (Dynal Biotech ASA). To purify CD4$^+$ or CD8$^+$ T lymphocytes, NKT cells expressing CD4 or CD8 were removed. DX5-negative cells were removed using anti-CD4 or anti-CD8α magnetic microbeads (Miltenyi Biotec GmbH). The magnetically labeled cells were purified by using VarioMACS system (Miltenyi Biotec GmbH). The isolated cells were served for the analysis of cytokine mRNA expression by real-time PCR.

*Real-time reverse transcription–PCR*

Total RNA was isolated and transcribed into complementary DNA (cDNA) using an RNeasy Mini Kit and an Omniscript Reverse Transcriptase Kit (QIAGEN GmbH, Hilden, Germany). The resulting cDNA was used as a template for real-time PCR along with primer–probe sets for the IL-2, IL-4, IFN-β, IFN-γ, TNF-α and CD40L (TaqMan Gene Expression Assays; Applied Biosystems, Foster City, CA, USA) and 2× Taqman universal PCR master mix (Applied Biosystems) according to the manufacturer's recommendations. IFN-α mRNAs were detected using SYBR Green reverse transcription (RT)–PCR. Primer–probe sets for 18S were used as an internal control in each reaction (Applied Biosystems). Real-time PCR data were analyzed using sequence detector software (Applied Biosystems).

*Intracellular cytokine staining*

For intracellular staining, the splenocytes from the mice administrated with HBsAg and α-GalCer were incubated for 4 h with brefeldin A (10 μg ml$^{-1}$). Then, cells were fixed and permeabilized with the Cytofix/Cytoperm buffer (BD PharMingen) and stained with PE-conjugated anti-mouse IFN-γ (clone XMG1.2), FITC-conjugated anti-mouse IL-4 (clone BVD6-24G2), PE-conjugated anti-mouse IL-2 (clone JES6-5H4) and PE-conjugated anti-mouse TNF-α (clone MP6-XT22) (eBioscience). Samples were acquired on a FSCStar flow cytometer and data analysis was conducted using CellQuest software (BD PharMingen).

*Statistics*

Values are expressed as means ± SEMs. Differences between experimental and control groups were analyzed by the Kruskal–Wallis test followed by Scheffe's *F*-test. Significance was established at $P < 0.05$.

## Results

*Effect of NKT cell activation on the efficiency of HBsAg-specific CTL induction*

Since it is well known that activated Vα14$^+$ NKT cells strongly produce T$_h$1 and two cytokines, we expected that this cell fraction can affect CTL induction. To determine if Vα14$^+$ NKT cells contribute to the induction of HBsAg-specific CTLs, we immunized Jα18$^{+/+}$ [wild-type (WT)] mice and Jα18$^{-/-}$ (KO) mice with i.p. injection of HBsAg and/or α-GalCer. It is well known that the efficiency of HBsAg-specific CTL induction is higher in HBV DNA immunization than in the immunization with HBsAg protein (17). However, considering further clinical application in human, we decided to use HBsAg protein for the immunization to induce HBsAg-specific CTLs. We examined HBsAg-specific lysis of CTL lines from Jα18 WT mice (Fig. 1A). Injection of HBsAg alone induced 19.2 and 38.3% HBsAg-specific lysis at an effector to target cell ratio

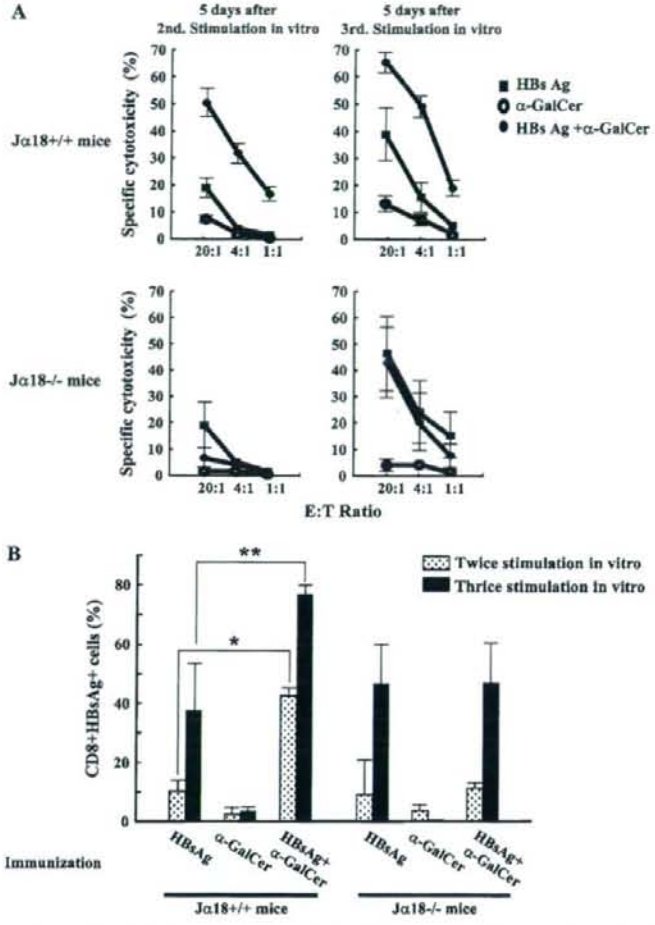


**Fig. 1.** HBsAg-specific cytolytic activity and HBsAgS28–39 specificity in the cell lines from immunized Jα18 WT and Jα18 KO mice. Jα18 WT or Jα18 KO mice were immunized with HBsAg (10 μg per mouse), α-GalCer (1 μg per mouse) or both. Splenocytes from these mice were prepared 7 days after immunization and were incubated with MMC-treated preS1-transfected P815 cells. (A) For the assay, effector cells (splenocytes) were incubated for 4 h with Eu-labeled target cells (P815 cells and preS1-transfected P815 cells) at an effector to target cell ratio of 20:1, 4:1 or 1:1. The percent specific cytotoxicity was calculated by subtracting the percent cytotoxicity of effector cells for P815 cells (HBsAg negative) from that for preS1-transfected P815 cells (HBsAg positive). Spontaneous release was always <20% of the total. Each data point and error bar represent the mean and the SEM, respectively, of results for triplicate samples. (B) Induction of HBsAg-specific $CD8^+$ cell responses was assessed by flow cytometric analysis using fluorescent dimeric H-$2L^d$–HBsAgS28–39 complexes. FACS profiles of Jα281 WT and Jα18 KO mice receiving HBsAg, α-GalCer or both are shown, with mean percentages of HBsAg $dimer^+$ $CD8^+$ cells plotted for each treatment. Each bar and error bar represent the mean and the SEM, respectively, of results for triplicate samples. Difference of percentages of HBsAg $dimer^+$ $CD8^+$ cells in the presence or absence of α-GalCer are compared. $^*P < 0.01$, $^{**}P < 0.05$.

of 20:1 following two or three *in vitro* stimulations, respectively. Injection of HBsAg with α-GalCer markedly enhanced specific lysis (50.2 and 65.3% after two and three stimulations, respectively) against HBsAg, but α-GalCer alone did not induce HBsAg-specific CTL responses. This enhancement of the HBsAg-induced CTL response by α-GalCer was not observed in Jα18 KO mice (Fig. 1A).

Next, we examined CTL frequencies using recombinant soluble dimeric H-$2L^d$ Ig, which can be used to stain $CD8^+$ T cells that are reactive for the H-$2L^d$-binding peptide HBsAgS28–39 (Fig. 1B). After two or three *in vitro* stimulations, the HBsAg-specific $CD8^+$ T cell counts in CTL lines from Jα18 WT mice immunized with a combination of HBsAg and α-GalCer were higher than those from WT mice

immunized with HBsAg alone. Also, there was no HBsAg-specific $CD8^+$ T cell from splenocytes of mice immunized with α-GalCer alone. The results of the cytotoxicity assays and the frequency analyses of HBsAg-specific CTLs indicate that α-GalCer strongly enhanced the induction and proliferation of HBsAg-specific CTLs in Jα18 WT mice.

*Cytokine and CD40L production by spleen in response to i.p. HBsAg and α-GalCer in Jα18 WT and Jα18 KO*

Previous studies demonstrated that several cytokines play important roles in the induction and proliferation of antigen-specific CTLs. Therefore, we measured the mRNA levels for IL-2, IL-4, IFN-γ, TNF-α and CD40L in whole spleens from Jα18 WT rmice and Jα18 KO mice stimulated with HBsAg alone or a combination of HBsAg and α-GalCer (Fig. 2A). Using real-time RT-PCR, we found that the expression of IL-2, IL-4, IFN-γ and TNF-α mRNA in the splenocytes from Jα18 WT mice was enhanced by immunization with both HBsAg and α-GalCer but not with HBsAg alone. The enhancement of mRNA expression for these cytokines reached maximum levels ~7 h after immunization with HBsAg and α-GalCer. In contrast, the enhancement of cytokine mRNA expression was not observed in Jα18 KO mice. The mRNA expression of CD40L seemed to be constitutive both in Jα18 WT and KO mice. There was no significant change in the expression of CD40L in Jα18 WT and KO mice by the addition of α-GalCer during the observation period. Next, we measured protein production levels of cytokines in splenocytes after injection of HBsAg and α-GalCer by intracellular cytokine staining. The intracellular staining shown in Fig. 2(B) indicated that IL-2, IL-4, IFN-γ and TNF-α production of splenocyte increased after immunization of a combination

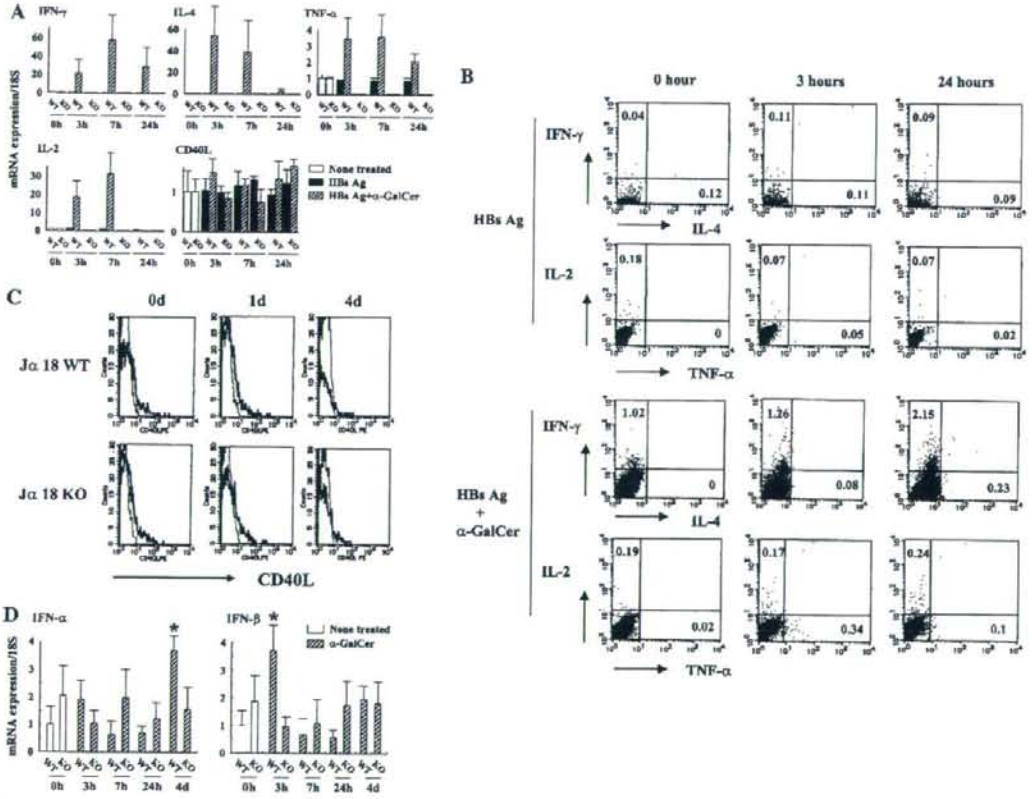


**Fig. 2.** Cytokine and CD40L production by spleen in response to i.p. HBsAg and α-GalCer. (A) Total spleen mRNA was prepared from Jα18 WT and KO mice immunized with HBsAg (10 μg per mouse) in the presence or absence of α-GalCer (1 μg per mouse) 3, 7 and 24 h after treatment. The expression of IL-2, IL-4, IFN-γ, TNF-α and CD40L mRNA was analyzed by real-time RT-PCR. (B) Flow cytometric analysis for intracellular cytokine produced by splenocytes taken from mice 0, 3 and 24 h after injection of HBsAg and α-GalCer, or HBsAg alone, and cultured for 4 h in brefeldin A. (C) CD40L expression on splenic CD3-positive cells 0 day, 1 day and 4 days after injection of HBsAg and α-GalCer. (D) The expression of IFN-α and IFN-β mRNA was analyzed by real-time RT-PCR. Results were normalized by the expression of 18S mRNA. Each bar and error bar represent the mean and the SEM, respectively, of results for triplicate samples. $^*P < 0.05$ compared with non-treated WT mice.

of HBsAg and α-GalCer. On the other hand, HBsAg-alone injection did not enhance the cytokine production in splenocytes. Furthermore, we examined the surface CD40L expression of splenocytes by flow cytometer. CD40L expression was not affected by the injection of α-GalCer as a result of real-time PCR (Fig. 2C).

Previous study demonstrated that α-GalCer activated intrahepatic NKT cells to secrete antiviral cytokines (IFN-γ and IFN-α/β) in the liver and had the potential to control viral replication during natural HBV infection (18). Therefore, we evaluated mRNA levels for IFN-α and IFN-β in whole spleens from Jα18 WT mice and Jα18 KO mice stimulated with α-GalCer (Fig. 2D). IFN-α mRNA expression level significantly was elevated 4 days after the immunization of α-GalCer. On the other hand, IFN-β mRNA expression level was rapidly increased after α-GalCer injection.

*Roles of IL-2, IL-4, IFN-γ, TNF-α and CD40L on the induction of CTLs*

We tested the effect of neutralizing antibodies to IL-2, IL-4, IFN-γ, TNF-α and CD40L on the induction of HBsAg-specific CTLs from Jα18 WT mice immunized with both HBsAg and α-GalCer. As shown in Fig. 3, the frequency of HBsAg-specific CTLs from mice immunized with HBsAg and α-GalCer was reduced by the administration of antibodies to IL-2 and CD40L. Although antibodies to IL-4 and TNF-α reduced the frequency of HBsAg-specific CTLs from mice immunized with HBsAg alone, these antibodies did not affect the frequency from mice immunized with both HBsAg and α-GalCer.

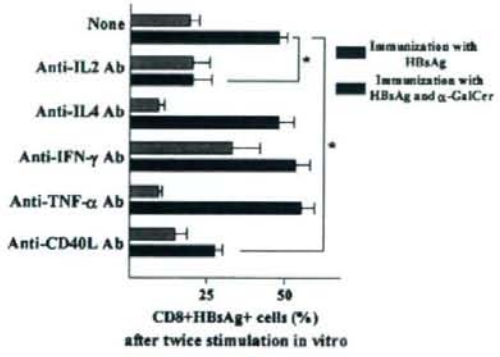


**Fig. 3.** Effect of IL-2, IL-4, IFN-γ, TNF-α and CD40L on the induction of HBsAg-specific CTLs. Jα18 WT mice were injected with neutralizing antibodies to IL-2, IL-4, IFN-γ, TNF-α or CD40L and then immunized with HBsAg (10 μg per mouse) in the presence or absence of α-GalCer (1 μg per mouse). Splenocytes prepared 7 days after immunization were incubated with MMC-treated P815/preS1 transfectants. Induction of HBsAg-specific $CD8^+$ cell responses was assessed by flow cytometric analysis using fluorescent dimeric $H\text{-}2L^d$–HBsAgS28–39 complexes. FACS profiles of mice receiving HBsAg or both HBsAg and α-GalCer are shown, with mean percentages of HBsAg dimer$^+$ $CD8^+$ cells plotted for each treatment group. Each bar and error bar represent the mean and the SEM, respectively, of results for triplicate samples. Difference of percentages of HBsAg dimer$^+$ $CD8^+$ cells in the presence or absence of neutralizing antibodies are compared. $^*P < 0.05$.

Next, we tested if co-administration of IL-2 and CD40L can substitute the enhancing effect of α-GalCer on CTL induction. Recombinant IL-2 and CD40L were co-administrated with HBsAg, and cytotoxicity of HBsAg-specific CTL lines and the frequency of HBsAg-specific CTLs were analyzed. After single stimulation *in vitro*, HBsAg-specific cytotoxicity of CTL lines from the mice immunized with HBsAg and α-GalCer was equal to that from mice immunized with IL-2, CD40L and HBsAg. The frequency of HBsAg-specific $CD8^+$ T cells in CTL lines from the mice immunized with IL-2, CD40L and HBsAg was rather higher than that from the mice immunized by the different protocols (Fig. 4).

It was recently reported that repeated stimulation of Vα14 NKT cells with α-GalCer treatments led to a change in their cytokine profile (19). We evaluated the effect of repeated stimulation of VαNKT cells with α-GalCer on the induction of HBsAg-specific CTLs and IL-2 production in Jα18 WT mice. Jα18 WT mice were immunized with HBsAg, HBsAg and once injection of α-GalCer or HBsAg and three times injection of α-GalCer. Induction of HBsAg-specific $CD8^+$ T cell responses was assessed by flow cytometric analysis. The frequency of HBsAg-specific $CD8^+$ T cells in CTL lines from the mice immunized with HBsAg and once α-GalCer was higher than that from the mice immunized by the other protocols (Fig. 5A). Furthermore, we found that the expression of IL-2 mRNA in the splenocytes from Jα18 WT mice was enhanced by immunization with once α-GalCer injection but not three times α-GalCer injection *in vivo* (Fig. 5B).

*Cytokine mRNA expression of splenic Vα14$^+$ NKT, CD4$^+$ T cells and CD8$^+$ T cells from Jα18 WT mice immunized with HBsAg and α-GalCer*

Next, we isolated Vα14$^+$ NKT, $CD4^+$ $DX5^-$ and $CD8^+$ $DX5^-$ cells from whole splenocytes by immunomagnetic separation and then examined which cell fractions produced these cytokines in the mice immunized with HBsAg and α-GalCer (Fig. 6). The expression of IFN-γ mRNA was enhanced in all the cell fractions, especially in Vα14$^+$ NKT and in $CD8^+$ T cells. IL-2 mRNA expression was also enhanced in all the fractions; however, the highest enhancement was observed in $CD4^+$ T cells. The enhancement of IL-4 mRNA expression was seen in Vα14$^+$ NKT and $CD4^+$ T cells. TNF-α mRNA expression was enhanced in $CD8^+$ T cells but not in Vα14$^+$ NKT and $CD4^+$ T cells. CD40L mRNA was expressed constitutively in $CD4^+$ T cells but not in Vα14$^+$ NKT or $CD8^+$ T cells. The expression level of CD40L was not changed by the addition of α-GalCer.

*Induction of HBsAg-specific CTLs in HBsAg transgenic mice*

HBsAg transgenic mice, which are immunologically tolerant to HBV-encoded antigens, are a model of chronic HBV infection (20). In order to test the possibility for inducing HBsAg-specific CTLs even in conditions of chronic HBV infection, we evaluated the HBsAg-specific CTL activity of harvested spleen cells from transgenic mice immunized with HBsAg or both HBsAg and α-GalCer following two or three *in vitro* stimulations with the P815preS1 transfectants. As shown in Fig. 7(A), HBsAg-specific cytotoxicity was induced only in mice immunized with both HBsAg and α-GalCer; CTL activity was not observed in spleen cells from the mice immunized with either HBsAg or α-GalCer alone. Furthermore,

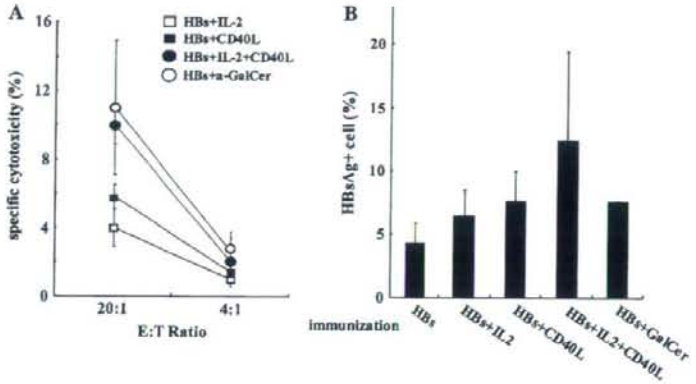


**Fig. 4.** Role of IL-2 and CD40L on the induction of HBsAg-specific CTLs. Jα18 WT mice were administrated ($4 \times 10^4$ U per mouse) or CD40L (100 μg per mouse) or both of IL-2 ($4 \times 10^4$ U per mouse) and CD40L (100 μg per mouse) or α-GalCer (1 μg per mouse) with HBsAg (10 μg per mouse). Splenocytes from these mice were prepared 7 days after immunization and were incubated with MMC-treated preS1-transfected P815 cells. (A) For the assay, effector cells were incubated for 4 h with Eu-labeled target cells (P815 cells and preS1-transfected P815 cells) at an effector to target cell ratio of 20:1 or 4:1. The percent specific cytotoxicity was calculated by subtracting the percent cytotoxicity of effector cells for P815 cells from that for preS1-transfected P815 cells. Each data point and error bar represent the mean and the SEM, respectively, of results for triplicate samples. (B) Induction of HBsAg-specific $CD8^+$ cell responses was assessed by flow cytometric analysis using fluorescent dimeric H-$2L^d$–HBsAgS28–39 complexes. Each bar and error bar represent the mean and the SEM, respectively, of results for triplicate samples.

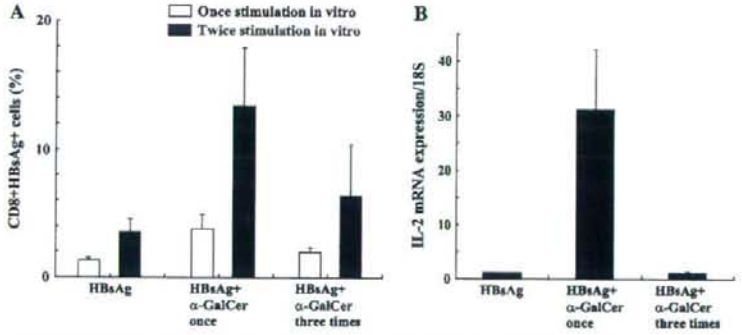


**Fig. 5.** Effect of repeated stimulation of VαNKT cells with α-GalCer on the induction of HBsAg-specific CTLs in Jα18 WT mice. Jα18 WT mice were immunized with HBsAg (10 μg per mouse), HBsAg and once injection of α-GalCer (1 μg per mouse) or HBsAg and three times injection of α-GalCer at interval 3 days. (A) Splenocytes from these mice were prepared 10 days after immunization and were incubated with MMC-treated preS1-transfected P815 cells. Induction of HBsAg-specific $CD8^+$ cell responses were assessed by flow cytometric analysis using fluorescent dimeric H-$2L^d$–HBsAgS28–39 complexes. Each bar and error bar represent the mean and the SEM, respectively, of results for triplicate samples. (B) Total spleen mRNA was prepared from Jα18 WT mice immunized 7 h after last α-GalCer injection. The expression of IL-2 mRNA was analyzed by real-time RT-PCR. Each bar and error bar represent the mean and the SEM, respectively, of results for triplicate samples.

quantitative flow cytometric analysis revealed that HBsAg-specific $CD8^+$ T cells appeared in the HBsAg transgenic mice only when they were immunized with HBsAg and α-GalCer (Fig. 7B).

Next, we tried to induce HBsAg-specific CTL clones in HBsAg transgenic mice after immunization with a combination of HBsAg and α-GalCer. By limiting dilution, we established CTL clones with high cytolytic activity from HBsAg transgenic mice (Table 1).

*Analysis of HBsAg-specific CTL precursor frequency in HBsAg transgenic mice immunized with HBsAg and α-GalCer*

To quantitate the number of HBsAg-specific CTL precursors in the HBsAg transgenic mice immunized with HBsAg and α-GalCer *ex vivo*, we used a limiting dilution technique. The $CD8^+$ T cells isolated by immunomagnetic beads from immunized mice were seeded at three cells per well and stimulated weekly with irradiated autologous splenocytes and P815preS1 *in vitro*. After 2 weeks stimulation, the number of

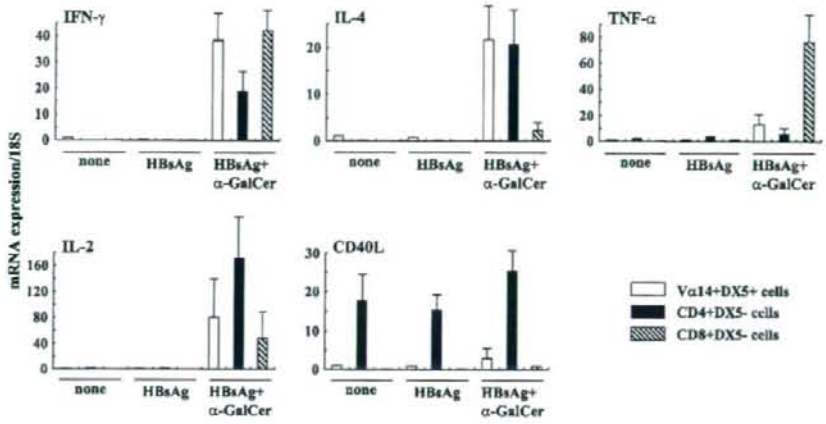


**Fig. 6.** Expression of IL-2, IL-4, IFN-γ, TNF-α and CD40L mRNA by splenic Vα14⁺ NKT, CD4⁺ or CD8⁺ cells from Jα18 WT mice immunized with HBsAg and α-GalCer. Jα18 WT mice were immunized with HBsAg (10 μg per mouse), α-GalCer (1 μg per mouse) or both. Splenic Vα14⁺ NKT, CD4⁺ and CD8⁺ cells were purified using immunomagnetic separation 7 h after treatment and used to prepare total mRNA. The expression of IL-2, IL-4, IFN-γ, TNF-α and CD40L mRNA was analyzed by real-time RT-PCR. Results were normalized by the expression of 18S mRNA.

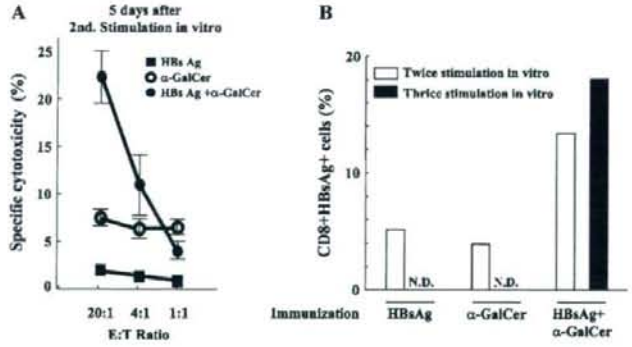


**Fig. 7.** Induction of HBsAg-specific CTLs in HBsAg transgenic mice immunized with HBsAg and α-GalCer. Cytotoxic activity of HBsAg-specific CTLs induced in HBsAg transgenic mice (A) and flow cytometric analysis of the frequency of HBsAg-specific CD8⁺ cells in HBsAg transgenic mice (B). HBsAg transgenic mice were immunized with HBsAg (10 μg per mouse), α-GalCer (1 μg per mouse) or both. Splenocytes prepared 7 days after inoculation were incubated with MMC-treated P815/preS1-transfected cells. Induction of HBsAg-specific CD8⁺ cell responses were assessed by a cytotoxic assay and flow cytometric analysis using dimeric H-2L$^d$–HBsAgS28–39 complexes. Each data point and error bar represent the mean and the SEM, respectively, of results for triplicate samples (A).

the wells with proliferating cells was counted and those cells were tested for HBsAg specificity. With the splenocytes from HBsAg transgenic mice immunized with HBsAg alone, the proliferation of the cells was observed only in four wells out of 960 wells, none of those cells showed specificity to HBsAgS28–39. In contrast, the proliferation was observed in 99 wells out of 960 wells, and 89% (88/99) of them showed HBsAgS28–39 specificity in the case of co-immunization with HBsAg α-GalCer (Table 2).

## Discussion

It is well known that CTLs play a key role not only in hepatocellular injury (6, 7) but also in viral clearance (8, 9). On the other hand, a lack of or a weak CTL response is observed in individuals with chronic HBV infection, and it is considered to be one of the main reasons for the persistence of HBV infection (1). Recent studies revealed that DNA vaccination and dendritic cell (DC) immunization overcome the tolerance of CTLs to autoantigens (17, 21) and tumors (22, 23). In HBsAg transgenic mice, repetitive immunization with a recombinant vaccinia virus encoding HBsAg breaks the tolerance at the B cell level but not the T cell level (20). Furthermore, an artificially synthesized peptide that includes specific epitopes for helper T lymphocytes and CTLs has been shown to break CTL tolerance in HBV transgenic mice (24). To attempt breaking CTL tolerance by modifying

**Table 1.** Cytotoxicity of clones from HBV transgenic mice immunized with HBsAg and α-GalCer

| | Mouse | Specific cytotoxicity (%) | |
|---|---|---|---|
| | | E:T = 20:1 | E:T = 4:1 |
| Clone T-1 | Transgenic | 42.2 | 21.8 |
| Clone T-2 | Transgenic | 17.8 | 10.5 |
| Clone T-3 | Transgenic | 36.8 | 2.5 |

HBsAg-specific CTL clones were established by limiting dilution and the cytolytic activity of HBsAg specific was assessed using a Europium release assay. The details are described in Methods.

**Table 2.** Analysis of HBsAg-specific CTL precursor frequency

| Mouse | Immunization | Rate of cell proliferation | HBsAg positive |
|---|---|---|---|
| HBV Tg | HBsAg | 4/960 | 0/4 |
| HBV Tg | HBsAg + α-GalCer | 99/960 | 88/99 |

The CD8-positive cells (three cells per well) isolated by using MACS system were cultured in 96-well plates with MMC-treated spleen cells ($4 \times 10^5$ per well) and MMC-treated P815preS1 ($2 \times 10^4$ per well) in complete RPMI 1640. The cells were re-stimulated with MMC-treated spleen cells and P815preS1 every 7 days. After 14 days, the number of wells in which the cells proliferated was counted and the proportion of HBsAg-specific CTLs was measured by flow cytometric analysis on a FACScan.

immunization method and to elucidate its mechanisms for the tolerance break, studies need to be performed under physiological conditions. Therefore, we performed the experiments using HBsAg transgenic mice, the model of the HBV carriers.

Previous study demonstrated that α-GalCer activated intrahepatic NKT cells to secrete antiviral cytokines (IFN-γ and IFN-α/β) in the liver and had the potential to control viral replication during natural HBV infection (18). Recently, another studies reported that antigen-specific CTLs were remarkably induced when antigen was administrated together with α-GalCer by the intra-nasal route (25, 26). Therefore, we evaluated the effect of activated NKT cells on the induction of HBsAg-specific CTL by administering α-GalCer. Indeed, we found that the activation of Vα14$^+$ NKT cells by α-GalCer strongly enhanced the efficiency of CTL induction in the Vα14$^+$ NKT WT mice, whereas this did not occur in the Vα14$^+$ NKT KO mice. Frequency analysis clearly showed that activated Vα14$^+$ NKT cells increase the number of HBsAg-specific CD8$^+$ T cells. Furthermore, the enhancement of CTL induction efficiency was observed not only in non-transgenic mice but also in HBsAg transgenic mice.

After the immunization with HBsAg and α-GalCer, the elevation of serum alanine aminotransferase (ALT) was observed in HBsAg transgenic mice (ALT levels; 5061 ± 1071 IU l$^{-1}$) but not in non-transgenic mice. Furthermore, we confirmed no liver injury in Jα18 KO mice/HBsAg transgenic mice immunized with HBsAg and α-GalCer (data not shown). Thus, the activation of NKT cells induced the liver injury in HBsAg transgenic mice after α-GalCer injection. HBsAg transgenic mice (lineage 107-5D) used in this study are consistently more sensitive to LPS or inflammatory cytokine (i.e. IFN-γ and TNF-α) compared with other HBV Tg mice lineage (27). Therefore, severe liver injury in these HBsAg transgenic mice was caused by cytokines produced by α-GalCer-activated NKT cells. Other reports have indicated that α-GalCer was not toxic in human including liver injury (28–30). However, our data suggested the fear of severe liver injury in patients with chronic HBV infection. The kinetics of ALT, which started to rise just after the immunization and declined within several days, also supports the idea above. The CTLs induced by the immunization might have the potential to cause liver damage. However, from the kinetics of ALT levels, it is unlikely that those CTLs contributed the ALT elevation in this case. It may be explained by HBsAg down-regulation, which was caused by the effect of IFN-γ and TNF-α (8, 9). Moreover, previous report demonstrated that HBV-specific CTLs profoundly suppress hepatocellular HBV gene expression in HBV transgenic mice by a non-cytolytic process (8, 9). Thus, the CTL induction was very meaningful for HBV clearance even if the destruction of the HBV-infected hepatocytes is induced by the CTLs. On the other hand, Mancini *et al.* (31) have reported that HBV DNA immunization successfully broke B- and T cell unresponsiveness to viral antigens in HBV transgenic mice, but these antigen-specific immune responses did not cause an increase in transaminase activity. We have not studied if this phenomenon is applicable in our model; however, further study including the detailed analysis of *in vitro* and *in vivo* function of CTLs induced from the tolerant mice will be necessary.

Next, we examined the effect of blocking cytokines and CD40L with neutralizing antibodies *in vivo*. Our results suggested that IL-4, TNF-α and CD40/CD40L are important for CTL induction in the case of HBsAg alone and that IL-2 and CD40L are essential for the enhancement of CTL induction in the case of HBsAg and α-GalCer co-immunization. In addition, it was proved that the enhancing effect of α-GalCer on CTL induction could be substituted by IL-2 and CD40L in the HBsAg immunization experiment. As shown in Fig. 5, the frequency of HBsAg-specific CD8$^+$ T cells in CTL lines and IL-2 production from the mice immunized with HBsAg and once α-GalCer was higher than those from the mice immunized with HBsAg and three times α-GalCer. These data indicated that the enhancement of IL-2 production is critical for CTL induction in the case of HBsAg and α-GalCer co-immunization.

In the splenocytes of the mice administered with α-GalCer, we found that the expression of cytokine mRNAs was strongly enhanced and that the enhancement of mRNA expression was observed not only in NKT cells but also in CD4$^+$ and CD8$^+$ T cells. IL-2 mRNA expression was enhanced in all the analyzed cell fractions. In particular, CD4$^+$ T cells mainly produced IL-2 in activation of NKT cells and expression of CD40L on CD4$^+$ T cells constitutively was important for CTL induction. It was previously reported that CTL responses require the activate involvement of CD4$^+$ T cells (32, 33). Moreover, activated NKT cells stimulate the full maturation of DCs, and this maturation accounts for the induction of combined $T_h1$ and CD8$^+$ T cell immunity to a co-administered protein (34).

As demonstrated previously (35), the administration of α-GalCer strongly enhanced the expression of mRNAs encoding cytokines, including IFN-γ, TNF-α, IL-2 and IL-4, which are known to affect CTL induction and proliferation (36–39). On the other hand, a CD40/CD40L signal is known to play a critical role in the NKT–DC interaction (40–42), and production of IFN-γ but not IL-4 by NKT cells requires a CD40/CD40L signal (42). It is also suggested that monocyte-derived DCs generated in the presence of IL-15 can express IL-2 on activation with CD40L. IL-2 and IL-15 are reported to play an important role in the acquired immune response to foreign pathogens (43). We think that our results are consistent with these reports and that they support our results that IL-2 and CD40–CD40L interaction play the key role on the induction of CTL response.

In the current studies, we showed that CTL tolerance in HBsAg transgenic mice can be broken by the activation of Vα14$^+$ NKT cells. Although the cytotoxic activity and proliferation of HBsAg-specific CTLs from the HBsAg transgenic mice were lower than those from WT mice, they were apparently induced in the transgenic mice. In addition, by using limiting dilution analysis, we confirm that HBsAg-specific CTL precursor cells are present relatively frequently in the spleen of HBsAg transgenic mice treated with HBsAg and α-GalCer. Persistent HBV infection is characterized by a lack of or a weak CTL response to HBV; however, our findings suggested that this weak CTL response can be enhanced or that CTL tolerance can be broken by the activation of NKT cells. We think that it can be applied to the therapeutic purpose, suppressing HBV replication by inducing effective CTL response. We also think that it may explain the mechanism for the development of CH from asymptomatic status in human HBV carriers.

We conclude that the activation of NKT cells strongly promotes the proliferation of HBsAg-specific CTLs through production of a high level of IL-2 and that this enables the induction of CTLs even in HBsAg transgenic mice. These results may open up a new method for clearing the virus from patients with persistent HBV infection.

**Acknowledgements**

We are grateful to Francis V. Chisari for providing HBsAg transgenic mice lineage 107-5D and the HBsAg-specific CD8$^+$ CTL clone 6C2.

**Abbreviations**

| | |
|---|---|
| ALT | alanine aminotransferase |
| ASC | asymptomatic carrier |
| cDNA | complementary DNA |
| CH | chronic hepatitis |
| DC | dendritic cell |
| α-GalCer | alpha-galactosylceramide |
| HBV | hepatitis B virus |
| KO | knockout |
| MMC | mitomycin C |
| RT | reverse transcription |
| TNF | tumor necrosis factor |
| WT | wild-type |

**References**

1 Boni, C., Penna, A., Ogg, G. S. *et al.* 2001. Lamivudine treatment can overcome cytotoxic T-cell hyporesponsiveness in chronic hepatitis B: new perspectives for immune therapy. *Hepatology.* 33:963.
2 Binder, D. and Kundig, T. M. 1991. Antiviral protection by CD8+ versus CD4+ T cells. CD8+ T cells correlating with cytotoxic activity *in vitro* are more efficient in antivaccinia virus protection than CD4-dependent IL. *J. Immunol.* 146:4301.
3 Eichelberger, M., Allan, W., Zijlstra, M., Jaenisch, R. and Doherty, P. C. 1991. Clearance of influenza virus respiratory infection in mice lacking class I major histocompatibility complex-restricted CD8+ T cells. *J. Exp. Med.* 174:875.
4 Hou, S., Doherty, P. C., Zijlstra, M., Jaenisch, R. and Katz, J. M. 1992. Delayed clearance of Sendai virus in mice lacking class I MHC-restricted CD8+ T cells. *J. Immunol.* 149:1319.
5 Chisari, F. V., Filippi, P., McLachlan, A. *et al.* 1986. Expression of hepatitis B virus large envelope polypeptide inhibits hepatitis B surface antigen secretion in transgenic mice. *J. Virol.* 60:880.
6 Ando, K., Moriyama, T., Guidotti, L. G. *et al.* 1993. Mechanisms of class I restricted immunopathology. A transgenic mouse model of fulminant hepatitis. *J. Exp. Med.* 178:1541.
7 Ando, K., Guidotti, L. G., Cerny, A., Ishikawa, T. and Chisari, F. V. 1994. CTL access to tissue antigen is restricted *in vivo*. *J. Immunol.* 153:482.
8 Guidotti, L. G., Ando, K., Hobbs, M. V. *et al.* 1994. Cytotoxic T lymphocytes inhibit hepatitis B virus gene expression by a noncytolytic mechanism in transgenic mice. *Proc. Natl Acad. Sci. USA.* 91:3764.
9 Guidotti, L. G., Ishikawa, T., Hobbs, M. V., Matzke, B., Schreiber, R. and Chisari, F. V. 1996. Intracellular inactivation of the hepatitis B virus by cytotoxic T lymphocytes. *Immunity* 4:25.
10 Ando, K., Hiroishi, K., Kaneko, T. *et al.* 1997. Perforin, Fas/Fas ligand, and TNF-alpha pathways as specific and bystander killing mechanisms of hepatitis C virus-specific human CTL. *J. Immunol.* 158:5283.
11 Gremion, C., Grabscheid, B., Wolk, B. *et al.* 2004. Cytotoxic T lymphocytes derived from patients with chronic hepatitis C virus infection kill bystander cells via Fas-FasL interaction. *J. Virol.* 78:2152.
12 Bendelac, A., Rivera, M. N., Park, S. H. and Roark, J. H. 1997. Mouse CD1-specific NK1 T cells: development, specificity, and function. *Annu. Rev. Immunol.* 15:535.
13 Makino, Y., Kanno, R., Ito, T., Higashino, K. and Taniguchi, M. 1995. Predominant expression of invariant V alpha 14+ TCR alpha chain in NK1.1+ T cell populations. *Int. Immunol.* 7:1157.
14 Cui, J., Shin, T., Kawano, T. *et al.* 1997. Requirement for Valpha14 NKT cells in IL-12-mediated rejection of tumors. *Science.* 278:1623.
15 Kita, H., Moriyama, T., Kaneko, T. *et al.* 1993. HLA B44-restricted cytotoxic T lymphocytes recognizing an epitope on hepatitis C virus nucleocapsid protein. *Hepatology.* 18:1039.
16 Cerny, A., McHutchison, J. G., Pasquinelli, C. *et al.* 1995. Cytotoxic T lymphocyte response to hepatitis C virus-derived peptides containing the HLA A2.1 binding motif. *J. Clin. Invest.* 95:521.
17 Schirmbeck, R., Bohm, W., Ando, K., Chisari, F. V. and Reimann, J. 1995. Nucleic acid vaccination primes hepatitis B virus surface antigen-specific cytotoxic T lymphocytes in nonresponder mice. *J. Virol.* 69:5929.
18 Kakimi, K., Guidotti, L. G., Koezuka, Y. and Chisari, F. V. 2000. Natural killer T cell activation inhibits hepatitis B virus replication *in vivo*. *J. Exp. Med.* 192:921.
19 Kojo, S., Seino, K., Harada, M. *et al.* 2005. Induction of regulatory properties in dendritic cells by Valpha14 NKT cells. *J. Immunol.* 175:3648.
20 Wirth, S., Guidotti, L. G., Ando, K., Schlicht, H. J. and Chisari, F. V. 1995. Breaking tolerance leads to autoantibody production but not autoimmune liver disease in hepatitis B virus envelope transgenic mice. *J. Immunol.* 154:2504.
21 Shimizu, Y., Guidotti, L. G., Fowler, P. and Chisari, F. V. 1998. Dendritic cell immunization breaks cytotoxic T lymphocyte tolerance in hepatitis B virus transgenic mice. *J. Immunol.* 161:4520.
22 Rice, J., Buchan, S., Dewchand, H., Simpson, E. and Stevenson, F. K. 2004. DNA fusion vaccines induce targeted epitope-specific CTLs against minor histocompatibility antigens from a normal or tolerized repertoire. *J. Immunol.* 173:4492.

23 Paczesny, S., Banchereau, J., Wittkowski, K. M., Saracino, G., Fay, J. and Palucka, A. K. 2004. Expansion of melanoma-specific cytolytic CD8+ T cell precursors in patients with metastatic melanoma vaccinated with CD34+ progenitor-derived dendritic cells. *J. Exp. Med.* 199:1503.
24 Sette, A. D., Oseroff, C., Sidney, J. *et al.* 2001. Overcoming T cell tolerance to the hepatitis B virus surface antigen in hepatitis B virus-transgenic mice. *J. Immunol.* 166:1389.
25 Ko, S. Y., Ko, H. J., Chang, W. S., Park, S. H., Kweon, M. N. and Kang, C. Y. 2005. Alpha-galactosylceramide can act as a nasal vaccine adjuvant inducing protective immune responses against viral infection and tumor. *J. Immunol.* 175:3309.
26 Youn, H. J., Ko, S. Y., Lee, K. A. *et al.* 2007. A single intranasal immunization with inactivated influenza virus and alpha-galactosylceramide induces long-term protective immunity without redirecting antigen to the central nervous system. *Vaccine.* 25:5189.
27 Gilles, P. N., Guerrette, D. L., Ulevitch, R. J., Schreiber, R. D. and Chisari, F. V. 1992. HBsAg retention sensitizes the hepatocyte to injury by physiological concentrations of interferon-gamma. *Hepatology.* 16:655.
28 Veldt, B. J., van der Vliet, H. J., von Blomberg, B. M. *et al.* 2007. Randomized placebo controlled phase I/II trial of alpha-galactosylceramide for the treatment of chronic hepatitis C. *J. Hepatol.* 47:356.
29 Giaccone, G., Punt, C. J., Ando, Y. *et al.* 2002. A phase I study of the natural killer T-cell ligand alpha-galactosylceramide (KRN7000) in patients with solid tumors. *Clin. Cancer Res.* 8:3702.
30 Ishikawa, A., Motohashi, S., Ishikawa, E. *et al.* 2005. A phase I study of alpha-galactosylceramide (KRN7000)-pulsed dendritic cells in patients with advanced and recurrent non-small cell lung cancer. *Clin. Cancer Res.* 11:1910.
31 Mancini, M., Hadchouel, M., Davis, H. L., Whalen, R. G., Tiollais, P. and Michel, M. L. 1996. DNA-mediated immunization in a transgenic mouse model of the hepatitis B surface antigen chronic carrier state. *Proc. Natl Acad. Sci. USA.* 93:12496.
32 Keene, J. A. and Forman, J. 1982. Helper activity is required for the *in vivo* generation of cytotoxic T lymphocytes. *J. Exp. Med.* 155:768.
33 Cardin, R. D., Brooks, J. W., Sarawar, S. R. and Doherty, P. C. 1996. Progressive loss of CD8+ T cell-mediated control of a gamma-herpesvirus in the absence of CD4+ T cells. *J. Exp. Med.* 184:863.
34 Fujii, S., Shimizu, K., Smith, C., Bonifaz, L. and Steinman, R. M. 2003. Activation of natural killer T cells by alpha-galactosylceramide rapidly induces the full maturation of dendritic cells *in vivo* and thereby acts as an adjuvant for combined CD4 and CD8 T cell immunity to a coadministered protein. *J. Exp. Med.* 198:267.
35 Ito, H., Ando, K., Nakayama, T. *et al.* 2003. Role of Valpha 14 NKT cells in the development of impaired liver regeneration *in vivo*. *Hepatology.* 38:1116.
36 Kasahara, S., Ando, K., Saito, K. *et al.* 2003. Lack of tumor necrosis factor alpha induces impaired proliferation of hepatitis B virus-specific cytotoxic T lymphocytes. *J. Virol.* 77:2469.
37 Bachmann, M. F., Schorle, H., Kuhn, R. *et al.* 1995. Antiviral immune responses in mice deficient for both interleukin-2 and interleukin-4. *J. Virol.* 69:4842.
38 Widmer, M. B. and Grabstein, K. H. 1987. Regulation of cytolytic T-lymphocyte generation by B-cell stimulatory factor. *Nature.* 326:795.
39 Farrar, W. L., Johnson, H. M. and Farrar, J. J. 1981. Regulation of the production of immune interferon and cytotoxic T lymphocytes by interleukin 2. *J. Immunol.* 126:1120.
40 Hayakawa, Y., Takeda, K., Yagita, H., Van Kaer, L., Saiki, I. and Okumura, K. 2001. Differential regulation of Th1 and Th2 functions of NKT cells by CD28 and CD40 costimulatory pathways. *J. Immunol.* 166:6012.
41 Nishimura, T., Kitamura, H., Iwakabe, K. *et al.* 2000. The interface between innate and acquired immunity: glycolipid antigen presentation by CD1d-expressing dendritic cells to NKT cells induces the differentiation of antigen-specific cytotoxic T lymphocytes. *Int. Immunol.* 12:987.
42 Fujii, S., Liu, K., Smith, C., Bonito, A. J. and Steinman, R. M. 2004. The linkage of innate to adaptive immunity via maturing dendritic cells *in vivo* requires CD40 ligation in addition to antigen presentation and CD80/86 costimulation. *J. Exp. Med.* 199:1607.
43 Feau, S., Facchinetti, V., Granucci, F. *et al.* 005. Dendritic cell-derived IL-2 production is regulated by IL-15 in humans and in mice. *Blood.* 105:697.

Liver International ISSN 1478-3223

BASIC STUDIES

# Upregulation of indoleamine 2,3-dioxygenase in hepatocyte during acute hepatitis caused by hepatitis B virus-specific cytotoxic T lymphocytes *in vivo*

Naoki Iwamoto[1], Hiroyasu Ito[1], Kazuki Ando[1], Tetsuya Ishikawa[2], Akira Hara[3], Ayako Taguchi[3], Kuniaki Saito[4], Masao Takemura[1], Michio Imawari[5], Hisataka Moriwaki[6] and Mitsuru Seishima[1]

1 Department of Informative Clinical Medicine, Gifu University Graduate School of Medicine, Gifu, Japan
2 Cancer Immunotherapy Center, Nagoya Kyoritsu Hospital, Nakagawa, Nagoya, Japan
3 Department of Tumor Pathology, Gifu University Graduate School of Medicine, Gifu, Japan
4 Human Health Sciences, Graduate School of Medicine and Faculty of Medicine, Kyoto University, Sakyo, Kyoto, Japan
5 Second Department of Internal Medicine, Showa University School of Medicine, Shinagawa-ku, Tokyo, Japan
6 First Department of Internal Medicine, Gifu University Graduate School of Medicine, Gifu, Japan

**Keywords**
cytotoxic T lymphocyte – hepatitis B virus – indoleamine 2,3-dioxygenase

**Correspondence**
Dr. Hiroyasu Ito, Department of Informative Clinical Medicine, Gifu University Graduate School of Medicine, 1-1 Yanagido, Gifu 501-1194, Japan
Tel: +81 58 230 6430
Fax: +81 58 230 6431
e-mail: hito@gifu-u.ac.jp

Received 16 January 2008
Accepted 27 February 2008

DOI:10.1111/j.1478-3231.2008.01748.x

**Abstract**

*Background/Aims:* Indoleamine-2,3-dioxygenase (IDO) is a tryptophan-catabolizing enzyme inducing suppression of T-cell function and immune tolerance. In hepatitis B virus (HBV) transgenic (Tg) mice, the adoptive transfer of HBV-specific cytotoxic T lymphocytes (CTL) causes a necroinflammatory liver disease that is histologically similar to acute viral hepatitis in man. The present study aimed to determine IDO expression in the liver and hepatocytes during an acute hepatitis model. *Methods:* Serum L-kynurenine (L-Kyn) concentration in HBV Tg mice administered with HBV-specific CTL was measured over time, together with serum levels of alanine aminotransferase (ALT). Furthermore, we examined the expression of IDO in the total liver and isolated hepatocytes of HBV Tg mice after CTL injection using immunohistochemical analysis and reverse-transcription polymerase chain reaction (PCR). *Results:* In HBV Tg mice, HBV-specific CTL induced, over the course of several days, a chronic increase in serum L-Kyn levels, which was associated with a sustained enhancement of liver IDO activity. In particular, IDO expression was enhanced in the liver parenchymal cells (hepatocytes) after HBV-specific CTL injection both in immunohistochemical analysis and in reverse-transcription PCR. Moreover, murine recombinant interferon-γ (IFN-γ) directly increased the IDO expression in primary hepatocytes *in vitro*. *Conclusions:* Cytotoxic T lymphocytes transduction results in the upregulation of IDO, which might downregulate T-cell responsiveness. Our findings provide evidence that hepatocyte itself expresses IDO and increases levels of L-Kyn in the blood in acute lethal hepatitis of mice. These data indicate that HBV infection facilitates the induction of IDO in response to proinflammatory cytokines, particularly IFN-γ.

Fulminant hepatitis is a clinical syndrome consisting of sudden and severe liver dysfunction that causes hepatic encephalopathy and acute liver dysfunction (1). Fulminant hepatitis develops in about 1% of patients with acute hepatitis B (2) and its mortality remains high. Hepatitis B virus (HBV) is a nonlytic virus that does not cause direct infected cell damage (3). Liver damage and viral clearance after HBV infection are thought to be mediated by the host cellular immune response to viral antigens. A fulminant hepatitis model has been created in mice by adoptive transfer of HBV-specific cytotoxic T lymphocytes (CTL) into HBV transgenic (Tg) mice. This liver injury consists of three steps after the CTL injection (4). The mice develop a necroinflammatory liver disease that is histologically similar to acute viral hepatitis in man.

Indoleamine 2,3-dioxygenase (IDO) is an enzyme, ubiquitously distributed in mammalian tissues and cells, converting L-tryptophan (L-Trp) to *N*-formylkynurenine, which is further catabolized to L-kynurenine (L-Kyn). IDO is induced by interferon-γ (IFN-γ)-dependent and/or an independent mechanism and other pro-inflammatory cytokines in the course of an inflammatory response in cell types including macrophages, fibroblasts and epithelial cells (5, 6). Increased IDO activity provokes tolerance of antigen-presenting cells and deprives T cells of L-Trp, leading to proliferation arrest and T-cell apoptosis (7, 8). On the other hand, L-Kyn has been shown to act as an immunoregulatory molecule that mediates immunosuppressive effects in the tissue microenvironment. IDO activity contributes to maternal tolerance in pregnancy (9), control of allograft rejection (10) and protection against autoimmunity (11). IDO has been found in various tumours of different histotypes and increments in IDO activity correlate with tumour progression (12). Therefore, the activity of IDO might play an important role in the regulation of the immune response exerted by the antigen-presenting cells and also might provide transformed cells with a potent tool to escape the immune system assault. Furthermore, IDO activity in white

blood cells and in different organs significantly increases in the course of viral, microbial, fungal or other parasite infections and it has been proposed that this enzyme is an important component in the overall defense mechanism (13–16).

The activity of IDO in acute hepatitis has been poorly understood and no studies have attempted to confirm the induction of IDO in hepatocytes *in vivo*. We examined herein whether IDO expression in hepatocytes is induced during acute liver injury caused by HBV-specific CTL using HBV Tg mice.

## Materials and methods

### Mice

Male B10.D2 (H-2d) mice (age, 6–8 weeks; weight, 25–30 g) were obtained from Japan SLC Inc. (Shizuoka, Japan). HBV-Tg mice lineage 107-5D (official designation Tg [Alb-1, HBV] Bri66), (inbred B10.D2, H-2d), in which the HBV envelope coding region is under the control of the mouse albumin promoter, were generously provided by Dr Francis V. Chisari, Department of Molecular and Experimental Medicine, Scripps Research Institute, La Jolla, CA, USA. All procedures were conducted in accordance with the National Institutes of Health Guide for the Care and Use of Laboratory Animals, and with the guidelines for care and use of animals established by the Animal Care and Use Committee of Gifu University.

### Hepatitis B surface antigen-specific cytotoxic lymphocytes

Hepatitis B virus Tg mice were injected with a hepatitis B surface antigen (HBsAg)-specific, H-2d-restricted, $CD8^+$ CTL clone (designated 6C2) that recognizes an epitope (IPQSLDSWWTSL) located between residues 28 and 39 of HBsAg (4). At 5 days after the last stimulation, the cells were washed, counted and injected intravenously into HBV Tg mice.

### Induction and assessment of liver cell injury

$5 \times 10^6$ cells of the HBsAg-specific CTL clone 6C2 that we have previously shown (4) to induce severe Ag-dependent, major histocompatibility complex-class I-restricted liver cell injury in HBV envelope Tg mice were injected into the lateral tail vein in 200 μl of sterile saline. Before and at several time points, mice were bled by retro-orbital phlebotomy and the sera were analysed for the development of liver cell injury by measuring serum alanine aminotransferase activity (ALT). In selected experiments, hepatocellular injury and inflammation were confirmed by the examination of zinc formalin-fixed liver tissue sections stained with haematoxylin and eosin (HE).

### Determination of L-kynurenine concentrations

Plasma from the mice was mixed with three volumes of 3% perchloric acid, and tissue samples were sonicated in four volumes of 3% perchloric acid. After centrifugation, the concentrations of L-Kyn in the supernatants were measured using high-performance liquid chromatography (HPLC) with a 5-mm octyldecyl silane column (150 mm by 2.1 mm; Eicom, Kyoto, Japan) and a spectrophotometric detector or a fluorescence spectrometric detector as described previously (17). UV signals were monitored at 355 nm for L-Kyn. The mobile phase consisted of 2.5% acetonitrile in 0.1 M sodium acetate (pH 3.9) and was filtered through a 0.45-μm-pore-size HA-type filter obtained from Millipore Corp. (Bedford, MA, USA). The flow rate was maintained at 0.75 ml/min throughout the chromatographic run.

### Histopathological examination

Tissues were fixed in 10% formalin in phosphate-buffered saline overnight. Specimens were then embedded in paraffin. Three-micrometre sections were used for HE staining and IDO immunohistochemistry. For the immunohistochemistry, the deparaffinized sections were heated in 0.1 M citrate buffer (pH 6.0) using the Pascal® heat-induced target retrieval system (Dako, Carpinteria, CA, USA). Nonspecific antibody-binding sites were blocked in 0.01 M phosphate-buffered saline (PBS), pH 7.4, containing 2% bovine serum albumin (BSA; Wako, Osaka, Japan) for 60 min. Then the sections were incubated with rabbit anti-IDO polyclonal antibody (anti-mouse IDO antibody was generated by the peptide [H]-CMKPSKKKPTDGDKS-[OH]) 1:100 in 2% BSA/PBS and incubated overnight at 4 °C. Expression of the IDO protein was shown by the labelled streptavidin biotin (LSAB) method using the LSAB kit (Dako, Kyoto, Japan) containing biotinylated antibody and peroxidase-labelled streptavidin. The peroxidase-binding sites were detected by staining with 3,3′-diaminobenzidine. Finally, counterstaining was performed using Mayer's haematoxylin.

### Isolation of mouse hepatocytes

The abdomen of a sacrificed mouse was opened and a needle was inserted into the vena cava. The portal vein was punctured. The liver was perfused with PBS and liver perfusion medium (Invitrogen Life Technologies, Carlsbad, CA, USA). To obtain nonparenchymal cell (NPC) populations, the liver was perfused with liver digestion medium (Invitrogen Life Technologies), removed and gently pressed through a mesh. NPC populations were separated from parenchymal hepatocytes by centrifugation at 50 *g* for 5 min (18). The purified cell population obtained in the final cell pellet was composed of ≥96% hepatocytes as previously reported (19, 20).

### Quantification of indoleamine 2,3-dioxygenase mRNA by reverse-transcription and real-time polymersase chain reaction

Total RNA from tissues was rapidly isolated using an ISOGEN kit for RNA isolation (Nippon Gene, Tokyo, Japan). Total RNA (1 μg) was used for the synthesis of the first strand of cDNA. Reverse-transcription (RT)-polymerase chain reaction (PCR) was performed using an mRNA-selective PCR kit (Takara Biomedicals, Tokyo, Japan). The sample was reverse transcribed in a final volume of 50 μl at 50 °C for 30 min. The subsequent PCR was performed at 85 °C for 1 min, 55 °C for 1 min and 72 °C for 1 min. The final cycle was performed at 72 °C for 4 min. The nucleotide sequences for the forward and reverse primers for mouse IDO and β-actin were described previously (17). The final PCR products were electrophoresed on 2.5% agarose gels and visualized using UV light illumination after ethidium bromide staining. The resulting cDNA was used as a template for real-time PCR along with primer/probe sets for the IDO genes (TaqMan Gene Expression Assays; Applied Biosystems, Foster City, CA, USA) and 2 × Taqman universal PCR master mix (Applied Biosystems) according to the manufacturer's recommendations. Primer/probe sets for 18S were used as an internal control in each reaction (Applied Biosystems).

Real-time PCR data were analysed using sequence detector software (Applied Biosystems).

### Culture of hepatocytes

Isolated hepatocytes were cultivated in Dulbecco's modified Eagle's medium supplemented with 10% foetal bovine serum and were maintained at 37 °C in a humidified atmosphere of 95% air and 5% $CO_2$ as described previously (21). After 24 h, the medium was replaced with fresh medium containing cytokine. At this time, the cells adhered to the bottom and the murine recombinant IFN-γ was added to induce IDO. The medium was replaced with 0 and 500 U/ml IFN-γ, and then incubated for an additional 24 h.

### Data analysis

All data were expressed as means ± standard deviation (SD), and Student's *t*-test was used for the statistical analysis. Values were considered to be significantly different when the *P*-value was $< 0.05$.

## Results

### Hepatitis B virus-specific cytotoxic T lymphocytes induce an acutely fatal necroinflammatory liver disease (fulminant hepatitis) in Hepatitis B virus Tg Mice

Hepatitis B virus-specific $CD8^+$ CTL clone, designated 6C2, was used in this study because of its excellent cytotoxic and growth characteristics *in vitro*. Most studies were performed by the injection of clone 6C2 into lineage 107-5D. In this study, the severity of liver damage (evaluated by serum ALT levels) was greater in HBV Tg mice (6143 ± 1406 U/L) than in non-Tg littermate mice (39 ± 3 U/L) ($P < 0.001$) 24 h after administration of $5 \times 10^6$ CTL. Histological changes in the liver of HBV Tg mice were examined on days 0, 3 and 7 after HBV-specific CTL injection. A histological analysis revealed widely scattered necroinflammatory foci, containing mostly mononuclear cells and apoptotic hepatocytes in the liver after the CTL injection. On the other hand, non-Tg littermate mice were also examined histologically at the same time points after CTL injection. In non-Tg littermate mice, the invasion of a large amount of inflammatory cells and hepatocellular necrosis was not observed (data not shown).

### Immunohistopathological examination on the expression of indoleamine 2,3-dioxygenase in the liver

Next, in order to verify IDO expression in the liver, we stained the liver tissues with anti-mouse IDO monoclonal antibody after HBV-specific CTL injection. Immunohistopathological examination revealed that IDO expression was upregulated in the hepatocytes of HBV Tg mice 7 days after HBV-specific CTL injection (Fig. 1E, F). In particular, the increase in IDO expression was observed in the liver parenchymal cells around the central vein. On the other hand, an increase in IDO expression in the liver could not be confirmed in non-Tg littermate mice after the CTL injection (Fig. 1I, J). Moreover, we measured the IDO expression in the hepatocytes of HBV Tg mice 1 and 3 days after HBV-specific CTL injection. The weak increase in IDO expression was also observed in the hepatocytes 1 and 3 days after CTL injection (Fig. 2).

### Temporal profiles of indoleamine 2,3-dioxygenase induction in hepatitis B virus Tg mice injected with hepatitis B virus-specific cytotoxic T lymphocytes

We investigated the time course of changes in serum L-Kyn concentrations and mRNA expression in the liver of HBV Tg mice injected with HBV-specific CTL (Fig. 3 and Fig. 4A). Serum L-Kyn levels in HBV Tg mice were significantly increased at least as early as day 1 after CTL injection compared with non-Tg littermate mice (0.87 ± 0.28 versus 2.91 ± 0.92 μM; $P < 0.01$), and this increase in serum L-Kyn levels persisted on day 7 after CTL injection. The total liver IDO mRNA expression level in HBV Tg mice was increased on day 1 and day 3 after HBV-specific CTL injection (Fig. 4A). On the other hand, this enhancement of IDO expression was not observed in non-Tg littermate mice after CTL injection. Because immunohistopathological examination revealed that IDO expression was increased in the hepatocytes of HBV Tg mice after the CTL injection, we examined the IDO mRNA expression level in isolated hepatocytes alone from HBV Tg mice treated with CTL. The hepatocyte IDO mRNA expression level was markedly increased on day 1 after the CTL injection (Fig. 4B). Next, we measured IDO expression in the liver and hepatocytes by using the real-time PCR method (Fig. 4C). The increase of IDO expression in the hepatocytes of the HBV Tg mice was observed at 3 days after the CTL injection.

### The effect of interferon-γ on indolamine 2,3-dioxygenase expression in hepatocytes

Indolamine 2,3-dioxygenase is believed to be induced by an IFN-γ-dependent and/or independent mechanism and IFN-γ is known to be highly enhanced in the liver of HBV Tg mice after HBV-specific CTL injection. Therefore, we examined the direct IFN-γ effect on primary hepatocytes *in vitro*. As shown in Figure 5, the IDO mRNA expression level in nontreated primary hepatocytes was not increased, but murine recombinant IFN-γ induced the IDO mRNA expression in both primary hepatocytes of HBV Tg and non-Tg littermate mice.

## Discussion

In the present study, we have shown that the IDO expression in hepatocytes and serum L-Kyn concentration increased during the severe liver injury induced by HBV-specific CTL. This murine acute hepatitis model is thought to be similar to acute viral hepatitis in man (4). In the acute phase of this model, various cytokines, especially IFN-γ, are increased in the liver and many host inflammatory cells infiltrate the liver. Therefore, we speculated that IDO expression is enhanced during acute liver injury similar to acute viral hepatitis. Indeed, as shown in Figure 1, IDO expression in the liver of HBV Tg mice, in particular hepatocytes, was increased after HBV-specific CTL injection. Concurrently, an increase in serum L-Kyn concentration was observed during acute liver injury. In brief, this increase in the serum L-Kyn level can be explained by the enhancement of IDO expression in hepatocytes of HBV Tg mice administered CTL. The IDO mRNA expression in hepatocytes rapidly was enhanced after CTL injection and the enhancement was observed at 3 days after CTL injection (Fig. 4C). On the other hand, immunohistopathological examination revealed that IDO expression was slightly enhanced at 1 and 3 days after CTL injection and strongly enhanced at 7 days after CTL injection (Fig. 2). These data indicated that IDO

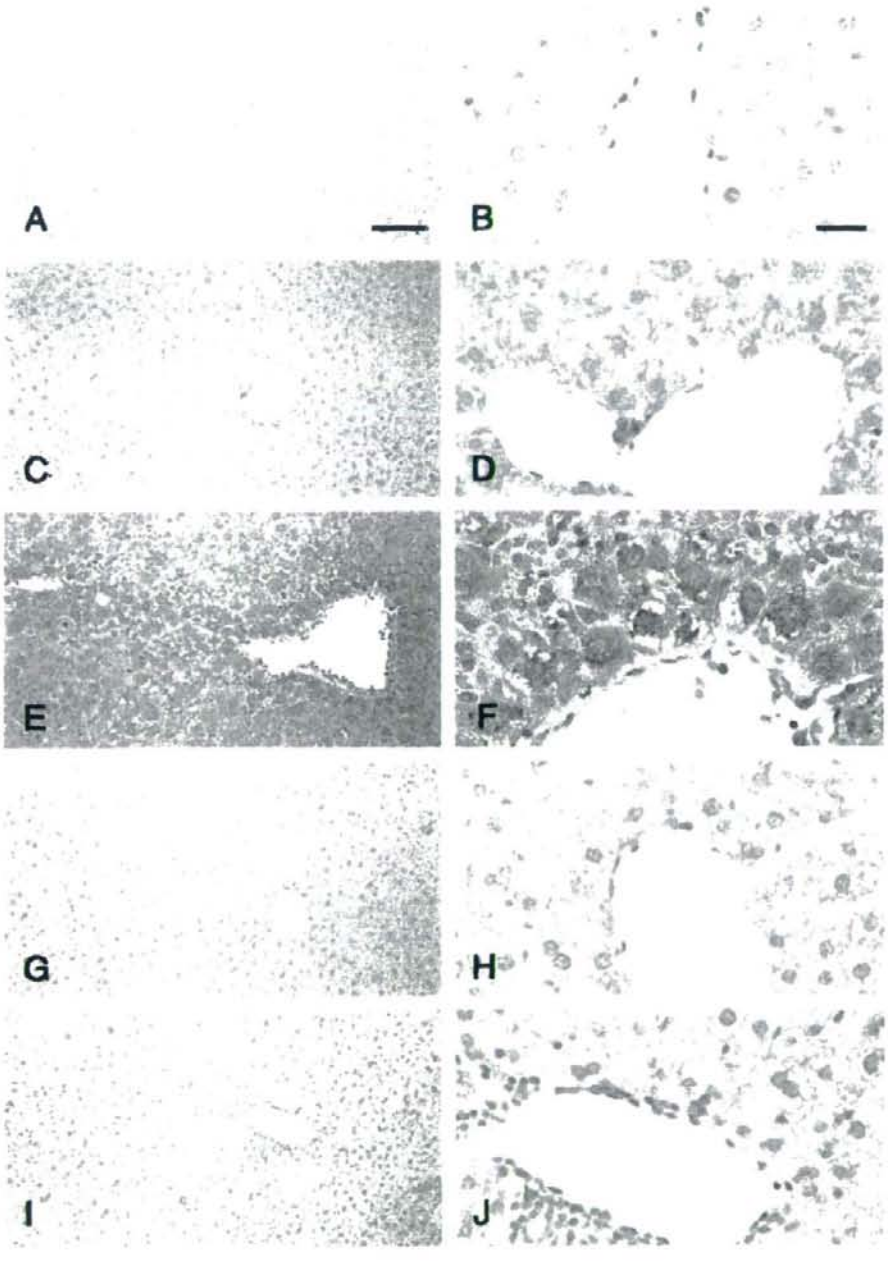



Liver International (2009)

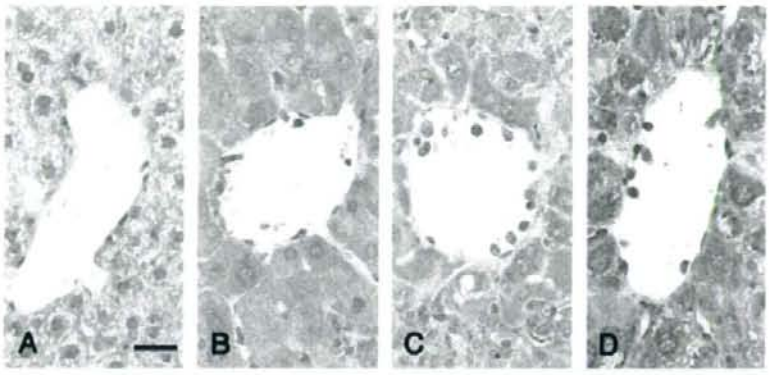


**Fig. 2.** Time-course of representative microphotographs of immunohistochemical staining for indole 2,3-dioxygenase in the liver tissues of a hepatitis B virus Tg mouse model on 0 (A), 1st (B), 3rd (C) and 7th (D) day after intravenous injection of cytotoxic T lymphocytes. Scale bar in panel A; 25 μm.

in hepatocytes may rapidly induce and stably exist for 7 days after CTL injection.

Most recently, it has been reported that IDO expression in the liver and serum kynurenine/tryptophan ratio in patients with chronic hepatitis C (HCV) were increased (15) and that this upregulation of IDO was caused by the IFN-γ produced by activated T cells in the liver with HCV. In the present study, we demonstrated that IDO expression in acute hepatitis is also enhanced, and confirmed that this enhancement was derived from hepatocytes. Therefore, it is likely that proinflammatory cytokine, such as IFN-γ, which is one of the inducing factor, is critical in the enhancement of IDO expression in hepatocytes during acute and chronic hepatitis.

The catabolism of L-Trp is differentially controlled during health and disease by two distinct enzymes: tryptophan 2,3-dioxygenase (TDO) and IDO. TDO is predominantly located in the liver and has a very strict substrate specificity, acting only on L-Trp (22), while IDO has a lower substrate specificity and is present in most mammalian cells including human mononuclear macrophages. Previous studies suggested that the activity of hepatocellular TDO decreased and IDO was induced in extrahepatic sites during inflammation and disease (23), resulting in the downregulation of L-Trp metabolism in the liver. However, our findings suggest that the IDO expression in hepatocytes was enhanced during acute hepatitis *in vivo*. As shown in Figure 5, the IDO expression in primary hepatocytes was induced by murine recombinant IFN-γ *in vitro*. In this acute hepatitis model, a large amount of IFN-γ is produced by HBV-specific CTL that directly contact HBsAg-positive hepatocytes (4, 24). Moreover, IFN-γ mRNA expression was upregulated at least 3–5 days after CTL injection in this murine acute hepatitis model (25). Therefore, it is assumed that the IDO expression in HBV Tg mice hepatocytes is enhanced in the early phase after HBV-specific CTL injection and the enhancement was sustained at 7 days after CTL injection. It was previously reported that bacterial lipopolysaccharide (LPS), a potent inducer of inflammatory cytokines *in vivo*, causes a severe acute liver disease in HBV Tg mice (26). We also examined the activity of IDO expression in hepatocytes when HBV Tg mice were administered LPS *in vivo*. The activity of IDO in hepatocytes was enhanced in LPS-induced liver injury just as in CTL-induced liver injury in HBV Tg mice (data not shown). It is thought that IFN-γ plays a critical role in these two models, and that the activity of IDO may be enhanced in IFN-γ-related liver injury.

Evidence accumulated over the last few years has indeed shown that the regulation of IDO expression and activity is an important event in the process leading to T lymphocyte proliferation and in the modulation of the immune responses (8, 27, 28). IDO activity contributes to maternal tolerance in pregnancy, control of allograft rejection, tumour progression and protection against autoimmunity (9, 29). In all these disorders, serum L-Trp concentrations are reduced while L-Kyn levels are elevated. Indeed, two major theories of L-Trp catabolism recently have been proposed to account for immune tolerance induction via L-Trp catabolism. One theory assumes that downstream metabolites of L-Trp catabolism, collectively known as L-Kyn, act to suppress immune reactivity, probably through direct interactions with effector T lymphocytes, natural killer (NK) cells and other cell types. The other theory posits that L-Trp itself has a key role and breakdown of this molecule suppresses T-cell proliferation by critically reducing

**Fig. 1.** Immunohistochemistry of indole 2,3-dioxygenase in the liver tissues of a hepatitis B virus (HBV) Tg mouse model on the seventh day after intravenous injection of cytotoxic T lymphocyte (CTL). (A, B) Liver tissue of negative control; (C, D) liver tissue before injection of CTL in HBV Tg mouse; (E, F) liver tissue 7 days after injection of CTL in HBV Tg mouse; (G, H) liver tissue before injection of CTL in non-Tg littermate mouse; (I, J) liver tissue 7 days after injection of CTL in non-Tg littermate mouse. A, C, E, G and I; low-power field of liver tissue, B, D, F, H and I; high-power field of view around the central vein. Scale bars in panel A; 100 μm and B; 25 μm. The severity of liver damage (evaluated by serum alanine transferase levels) was greater in HBV Tg mice (6143 ± 1406 U/L) than in non-Tg littermate mice (39 ± 3 U/L) ($P < 0.001$) 24 h after administration of $5 \times 10^6$ CTL.

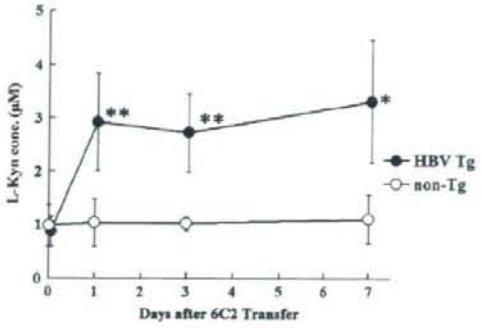


**Fig. 3.** High-performance liquid chromatography (HPLC) analysis of L-kynurenine (L-Kyn) concentrations in acute hepatitis of hepatitis B virus (HBV) Tg mice. L-Kyn concentrations in serum determined by HPLC method on HBV Tg mice after cytotoxic T lymphocytes injection. Significantly different from non-Tg, $^{*}P < 0.05$, $^{**}P < 0.01$.

the availability of the indispensable amino acid under local tissue microenvironments. Highly expressed IDO in hepatocytes during the early phase of fulminant hepatitis might enable the cells to initially avoid immune attack and then to reduce T-cell and/or NK-cell priming and the infiltration of effector inflammatory cells via local L-Trp depletion. In this study, the peculiarity of HBV Tg mice with CTL is that serum L-Trp level was constant regardless of high serum L-Kyn concentration and increased IDO activity in hepatocytes. Recently, it was reported that programmed cell death (PD)-1:PD-L1, a cell surface signaling molecule known to inhibit T-cell function, interactions did contribute to the suppression of IFN-γ production by HBV-specific CTLs (30). The enhancement of IDO expression in hepatocytes may also be one mechanism responsible for the suppression of IFN-γ production by HBV-specific CTLs in the liver. One way to address this issue in the future would be with an experimental model of acute hepatitis B in HBV Tg/IDO-knockout mice.

In conclusion, in liver injury caused by HBsAg-specific CTL in HBV Tg mice, IDO expression is increased in hepatocytes. These data indicate that HBV infection facilitates the induction of IDO in response to proinflammatory cytokines, particularly IFN-γ.

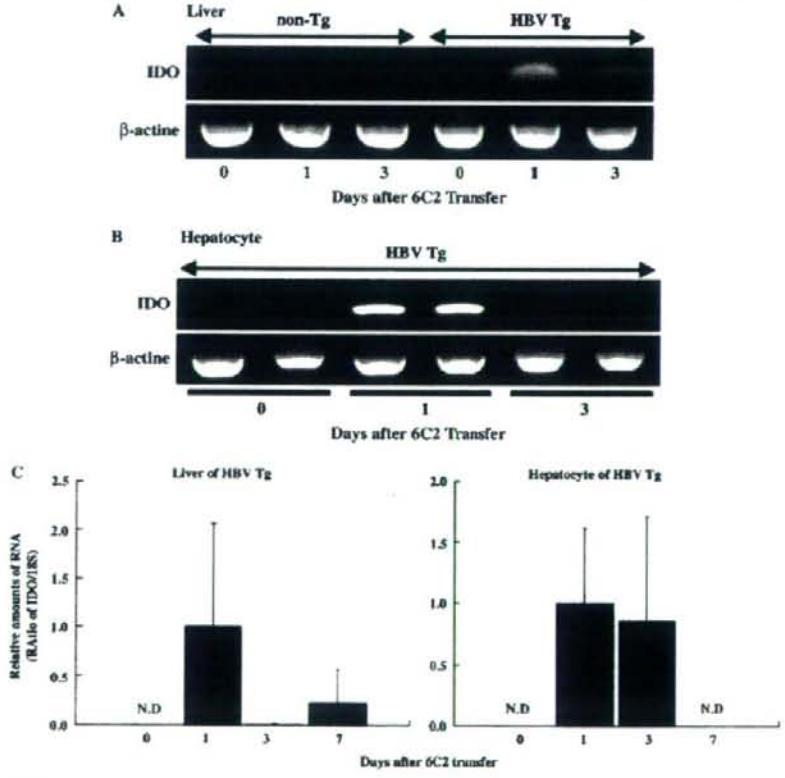


**Fig. 4.** Reverse-transcription (RT) polymerase chain reaction (PCR) analysis of indole 2,3-dioxygenase (IDO) mRNA expression in liver (A) and hepatocyte (B). Hepatitis B virus (HBV) Tg mice were injected with cytotoxic T lymphocytes (CTL). IDO mRNA levels were measured using RT-PCR. β-actin is shown as a loading control. PCR for β-actin was performed with the same cDNA samples. The relative expression levels of IDO mRNA in livers and hepatocytes on HBV Tg mice injected with CTL were measured using quantitative real-time PCR. Results were normalized by the expression of 18S mRNA (C). N. D.; not detected.


Liver International (2009)

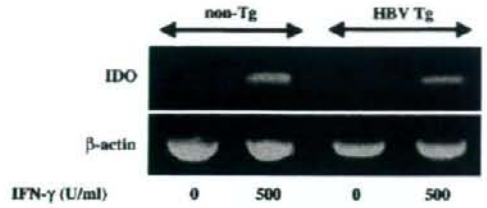


**Fig. 5.** Reverse-transcription polymerase chain reaction (PCR) analysis of indole 2,3-dioxygenase (IDO) mRNA expression in primary cultured hepatocytes from mice. Hepatocytes were cultivated in Dulbecco's modified Eagle's medium supplemented with 10% foetal bovine serum and maintained at 37 °C in a humidified atmosphere of 95% air and 5% $CO_2$. Hepatocytes were obtained from non-Tg littermate mice. After 24 h, the medium was replaced with fresh medium containing cytokine. At this time, the cells adhered to the bottom and interferon-γ (IFN-γ) was added to induce IDO. The medium was replaced with 0 and 500 U/ml IFN-γ, and then incubated for an additional 24 h.

## Acknowledgements

We thank Francis V. Chisari (The Scrips Research Institute) for providing the HBV transgenic mice and an HBsAg-specific $CD8^+$ CTL clone (designated 6C2). We express our gratitude to John Cole for reading our draft and giving us suggestions on language and style.

## References

1. Wright TL, Lau JY. Clinical aspects of hepatitis B virus infection. *Lancet* 1993; **342**: 1340–4.
2. Lettau LA, McCarthy JG, Smith MH, *et al.* Outbreak of severe hepatitis due to delta and hepatitis B viruses in parenteral drug abusers and their contacts. *N Engl J Med* 1987; **317**: 1256–62.
3. Chisari FV, Ferrari C. Hepatitis B virus immunopathology. *Springer Semin Immunopathol* 1995; **17**: 261–81.
4. Ando K, Moriyama T, Guidotti LG, *et al.* Mechanisms of class I restricted immunopathology, a transgenic mouse model of fulminant hepatitis. *J Exp Med* 1993; **178**: 1541–54.
5. Fujigaki S, Saito K, Sekikawa K, *et al.* Lipopolysaccharide induction of indoleamine 2,3-dioxygenase is mediated dominantly by an IFN-gamma-independent mechanism. *Eur J Immunol* 2001; **31**: 2313–8.
6. Murray HW, Szuro-Sudol A, Wellner D, *et al.* Role of tryptophan degradation in respiratory burst-independent antimicrobial activity of gamma interferon-stimulated human macrophages. *Infect Immun* 1989; **57**: 845–9.
7. Mellor AL, Munn DH. Tryptophan catabolism and T-cell tolerance: immunosuppression by starvation? *Immunol Today* 1999; **20**: 469–73.
8. Munn DH, Shafizadeh E, Attwood JT, Bondarev I, Pashine A, Mellor AL. Inhibition of T cell proliferation by macrophage tryptophan catabolism. *J Exp Med* 1999; **189**: 1363–72.
9. Mellor AL, Sivakumar J, Chandler P, *et al.* Prevention of T cell-driven complement activation and inflammation by tryptophan catabolism during pregnancy. *Nat Immunol* 2001; **2**: 64–8.
10. Grohmann U, Orabona C, Fallarino F, *et al.* CTLA-4-Ig regulates tryptophan catabolism *in vivo*. *Nat Immunol* 2002; **3**: 1097–101.
11. Grohmann U, Fallarino F, Bianchi R, *et al.* A defect in tryptophan catabolism impairs tolerance in nonobese diabetic mice. *J Exp Med* 2003; **198**: 153–60.
12. Huang A, Fuchs D, Widner B, Glover C, Henderson DC, Allen-Mersh TG. Serum tryptophan decrease correlates with immune activation and impaired quality of life in colorectal cancer. *Br J Cancer* 2002; **86**: 1691–6.
13. Fuchs D, Moller AA, Reibnegger G, Stockle E, Werner ER, Wachter H. Decreased serum tryptophan in patients with HIV-1 infection correlates with increased serum neopterin and with neurologic/psychiatric symptoms. *J Acquir Immune Defic Syndr* 1990; **3**: 873–6.
14. Yoshida R, Urade Y, Tokuda M, Hayaishi O. Induction of indoleamine 2,3-dioxygenase in mouse lung during virus infection. *Proc Natl Acad Sci USA* 1979; **76**: 4084–6.
15. Larrea E, Riezu-Boj JI, Gil-Guerrero L, *et al.* Upregulation of indoleamine 2,3-dioxygenase in hepatitis C virus infection. *J Virol* 2007; **81**: 3662–6.
16. Hissong BD, Byrne GI, Padilla ML, Carlin JM. Upregulation of interferon-induced indoleamine 2,3-dioxygenase in human macrophage cultures by lipopolysaccharide, muramyl tripeptide, and interleukin-1. *Cell Immunol* 1995; **160**: 264–9.
17. Fujigaki S, Saito K, Takemura M, *et al.* L-tryptophan-L-kynurenine pathway metabolism accelerated by *Toxoplasma gondii* infection is abolished in gamma interferon-gene-deficient mice: cross-regulation between inducible nitric oxide synthase and indoleamine-2, 3-dioxygenase. *Infect Immun* 2002; **70**: 779–86.
18. Ito H, Ando K, Nakayama T, *et al.* Role of V alpha 14 NKT cells in the development of impaired liver regeneration *in vivo*. *Hepatology* 2003; **38**: 1116–24.
19. Gregory SH, Wing EJ. IFN-gamma inhibits the replication of *Listeria monocytogenes* in hepatocytes. *J Immunol* 1993; **151**: 1401–9.
20. Gregory SH, Barczynski LK, Wing EJ. Effector function of hepatocytes and Kupffer cells in the resolution of systemic bacterial infections. *J Leukoc Biol* 1992; **51**: 421–4.
21. Heyes MP, Chen CY, Major EO, Saito K. Different kynurenine pathway enzymes limit quinolinic acid formation by various human cell types. *Biochem J* 1997; **326**(Pt 2): 351–6.
22. Schutz G, Beato M, Feigelson P. Messenger RNA for hepatic tryptophan oxygenase: its partial purification, its translation in a heterologous cell-free system, and its control by glucocorticoid hormones. *Proc Natl Acad Sci USA* 1973; **70**: 1218–21.
23. Takikawa O, Yoshida R, Kido R, Hayaishi O. Tryptophan degradation in mice initiated by indoleamine 2,3-dioxygenase. *J Biol Chem* 1986; **261**: 3648–53.
24. Yamasaki T, Handa H, Yamashita J, Watanabe Y, Namba Y, Hanaoka M. Specific adoptive immunotherapy of malignant glioma with long-term cytotoxic T lymphocyte line expanded in T-cell growth factor. Experimental study and future prospects. *Neurosurg Rev* 1984; **7**: 37–54.
25. Kakimi K, Lane TE, Wieland S, *et al.* Blocking chemokine responsive to gamma-2/interferon (IFN)-gamma inducible protein and monokine induced by IFN-gamma activity *in vivo* reduces the pathogenetic but not the antiviral potential of hepatitis B virus-specific cytotoxic T lymphocytes. *J Exp Med* 2001; **194**: 1755–66.
26. Gilles PN, Guerrette DL, Ulevitch RJ, Schreiber RD, Chisari FV. HBsAg retention sensitizes the hepatocyte to injury by physiological concentrations of interferon-gamma. *Hepatology* 1992; **16**: 655–63.
27. Frumento G, Rotondo R, Tonetti M, Damonte G, Benatti U, Ferrara GB. Tryptophan-derived catabolites are responsible for inhibition of T and natural killer cell proliferation induced by indoleamine 2,3-dioxygenase. *J Exp Med* 2002; **196**: 459–68.
28. Lee GK, Park HJ, Macleod M, Chandler P, Munn DH, Mellor AL. Tryptophan deprivation sensitizes activated T cells to apoptosis prior to cell division. *Immunology* 2002; **107**: 452–60.
29. Munn DH, Zhou M, Attwood JT, *et al.* Prevention of allogeneic fetal rejection by tryptophan catabolism. *Science* 1998; **281**: 1191–3.
30. Isogawa M, Furuichi Y, Chisari FV. Oscillating CD8 (+) T cell effector functions after antigen recognition in the liver. *Immunity* 2005; **23**: 53–63.

GASTROENTEROLOGY 2008;134:1396–1405

# Potential Relevance of Cytoplasmic Viral Sensors and Related Regulators Involving Innate Immunity in Antiviral Response

YASUHIRO ASAHINA,* NAMIKI IZUMI,* ITSUKO HIRAYAMA,* TOMOHIRO TANAKA,* MITSUAKI SATO,*,‡ YUTAKA YASUI,* NOBUTOSHI KOMATSU,*,‡ NAOKI UMEDA,* TAKANORI HOSOKAWA,* KEN UEDA,* KAORU TSUCHIYA,* HIROYUKI NAKANISHI,* JUN ITAKURA,* MASAYUKI KUROSAKI,* NOBUYUKI ENOMOTO,‡ MEGUMI TASAKA,§ NAOYA SAKAMOTO,§ and SHOZO MIYAKE*

*Department of Gastroenterology and Hepatology, Musashino Red Cross Hospital, Tokyo; ‡First Department of Internal Medicine, Faculty of Medicine, University of Yamanashi, Yamanashi; and §Department of Gastroenterology and Hepatology, Tokyo Medical and Dental University, Tokyo, Japan

***Background & Aims:*** **Clinical significance of molecules involving innate immunity in treatment response remains unclear. The aim is to elucidate the mechanisms underlying resistance to antiviral therapy and predictive usefulness of gene quantification in chronic hepatitis C (CH-C).** ***Methods:*** **We conducted a human study in 74 CH-C patients treated with pegylated interferon α-2b and ribavirin and 5 nonviral control patients. Expression of viral sensors, adaptor molecule, related ubiquitin E3-ligase, and modulators were quantified.** ***Results:*** **Hepatic RIG-I, MDA5, LGP2, ISG15, and USP18 in CH-C patients were up-regulated at 2- to 8-fold compared with non-hepatitis C virus patients with a relatively constitutive Cardif. Hepatic RIG-I, MDA5, and LGP2 were significantly up-regulated in nonvirologic responders (NVR) compared with transient (TR) or sustained virologic responders (SVR). Cardif and RNF125 were negatively correlated with RIG-I and significantly suppressed in NVR. Differences among clinical responses in RIG-I/Cardif and RIG-I/RNF125 ratios were conspicuous (NVR/TR/SVR = 1.3:0.6:0.4 and 2.3:1.3:0.8, respectively). Like viral sensors, ISG15 and USP18 were significantly up-regulated in NVR (4-fold and 2.3-fold, respectively). Multivariate and receiver operator characteristic analyses revealed higher RIG-I/Cardif ratio, ISG15, and USP18 predicted NVR. Lower Cardif in NVR was confirmed by its protein level in Western blot. Also, transcriptional responses in peripheral blood mononuclear cells to the therapy were rapid and strong except for Cardif in not only a positive (RIG-I, ISG15, and USP18) but also in a negative regulatory manner (RNF125).** ***Conclusions:*** **NVR may have adopted a different equilibrium in their innate immune response. High RIG-I/Cardif and RIG-I/RNF125 ratios and ISG15 and USP18 are useful in identifying NVR.**



Infection with hepatitis C virus (HCV) is a common cause of chronic hepatitis, which progresses to cirrhosis and hepatocellular carcinoma in many patients.[1] Although combination therapy with pegylated interferon (PEG-IFN) α and ribavirin is now established as the standard treatment for chronic HCV infection genotype 1b, the sustained virologic response rate in these patients is still around 50%.[2–4] Moreover, physicians have also found that 20% of patients are nonvirologic responders (NVR; those whose HCV-RNA does not become negative during 48 weeks of combination therapy).[5] Prediction of NVR status is of clinical importance because these patients have no chance of achieving a sustained virologic response even after prolonged combination therapy.[6] However, mechanisms involving resistance to PEG-IFN-α and ribavirin have not been fully elucidated, and it is difficult to predict treatment responses before initiation of PEG-IFN-α and ribavirin combination therapy.

In vitro studies have suggested that an innate immune response in viral infection is an essential part of the host antiviral defense system.[7] HCV evades the host immune response through a complex combination of processes that include signaling interference, effector modulation, and continual viral genetic variation.[8] We hypothesized that liver tissue would show a consistent difference between responders and nonresponders in expression levels of the gene involved in innate immunity and IFN signal transduction. These differences could be used to predict treatment outcomes.

The retinoic acid–inducible gene I (RIG-I), a cytoplasmic RNA helicase, and the related melanoma differentia-

*Abbreviations used in this paper:* CARD, Caspase-recruiting domain; Cardif, caspase-recruiting domain adaptor inducing IFN-β; G3PDH, glyceraldehyde-3-phosphate dehydrogenase; HCV, hepatitis C virus; IPS-1, IFN-β promoter stimulator I; ISG15, IFN-stimulated gene 15; PEG-IFN, pegylated interferon; MDA5, melanoma differentiation associated gene 5; MAVS, mitochondrial antiviral signaling protein; NVR, nonvirologic responders; PBMC, peripheral blood mononuclear cell; RIG-I, retinoic acid-inducible gene I; RNF125, ring-finger protein 125; ROC, receiver operator characteristic; SVR, sustained viral responder; TR, transient responder; UBP43, ubiquitin-specific protease 43; USP18, ubiquitin-specific protease 18; VISA, virus-induced signaling adaptor.


0016-5085/08/$34.00
doi:10.1053/j.gastro.2008.02.019

**Table 1.** Patient Characteristics at Baseline According to Final Virologic Response

| | SVR n = 30 | TR n = 24 | NVR n = 20 | *P* value |
|---|---|---|---|---|
| Age (*y*) | 52 ± 13 | 60 ± 8.7 | 60 ± 10 | .04[a] |
| Female % (M/F) | 47% (16/14) | 63% (9/15) | 60% (8/12) | .5[b] |
| Naïve & Relapser[c]/Non-responder[c] | 26/4 | 20/4 | 14/6 | .3[b] |
| BMI | 24.6 ± 3.0 | 24.9 ± 4.4 | 24.0 ± 2.1 | .6[a] |
| ALT (*IU/L*) | 75 ± 57 | 65 ± 35 | 68 ± 41 | 1.0[a] |
| Hemoglobin (*g/dL*) | 14.3 ± 1.6 | 14.1 ± 1.1 | 14.5 ± 1.7 | .6[a] |
| Platelet count ($\times 10^3/\mu L$) | 182 ± 62 | 169 ± 48 | 140 ± 39 | .04[a] |
| Liver histology | | | | |
| A1/A2/A3 | 19/8/3 | 14/8/1 | 10/10/0 | .3[b] |
| F1/F2/F3 | 14/9/7 | 11/7/5 | 7/5/8 | .7[b] |
| Viral load ($\times 10^6$ *IU/mL*) | 1.6 ± 1.2 | 1.8 ± 1.1 | 1.6 ± 1.1 | .8[a] |
| Viral decline rate ($log_{10}$/day) | | | | |
| First phase | 2.1 ± 0.9 | 1.5 ± 0.6 | 0.7 ± 0.5 | <.0001[a] |
| Second phase | 0.05 ± 0.05 | 0.04 ± 0.02 | 0.006 ± 0.008 | <.0001[a] |

ALT, alanine aminotransferase; BMI, body mass index.
[a]*P* values were determined by Kruskal–Wallis test.
[b]*P* values were determined by chi-square test.
[c]Response to previous IFN treatment.

tion-associated gene 5 (MDA5) play essential roles in initiating the host antiviral response by detecting intracellular viral dsRNA.[9,10] Caspase-recruiting domain (CARD) adaptor inducing IFN-$\beta$ (Cardif), also called IFN-$\beta$ promoter stimulator 1 (IPS-1), mitochondrial antiviral signaling protein (MAVS), and virus-induced signaling adaptor (VISA), is an adaptor molecule. Cardif connects RIG-I sensing to downstream signaling, resulting in IFN-$\beta$ gene activation.[11–14] On the other hand, RIG-I sensing has been shown to be negatively regulated in a dominant-negative manner by LGP2,[10,15] a helicase related to RIG-I and MDA5 lacking CARD. Interestingly, the ubiquitin ligase ring-finger protein 125 (RNF125) has been recently shown to conjugate ubiquitin to RIG-I, MDA5 as well as Cardif, which results in suppressing the functions of these proteins.[16] Furthermore, these molecules are conjugated (ISGylated) by IFN-stimulated gene 15 (ISG15), a ubiquitin-like protein,[17] and ISG15 is specifically removed from ISGylated protein by ubiquitin-specific protease 18 (USP18), also called ubiquitin-specific protease 43 (UBP43).[18,19] Moreover, the NS3/4A protease of HCV specifically cleaves Cardif as part of its immune evasion strategy.[11,20] Therefore, the RIG-I/Cardif system and its regulatory systems have essential key functions in the innate antiviral response (see Supplementary Figure 1 online at www.gastrojournal.org). However, the clinical significance of these innate immune systems, especially in relevance to the treatment response, is unclear because findings in this field have been mainly obtained by in vitro experiments using cell lines.

The aims of this study were to elucidate the mechanisms underlying resistance to antiviral therapy in the clinical setting and to determine whether quantification of transcripts of positive and negative cytoplasmic viral sensors and related regulatory molecules involving innate immune system is useful in predicting responses to PEG-IFN-$\alpha$ and ribavirin combination therapy.

## Patients and Methods

### *Patients*

Among patients with biopsy-proven chronic hepatitis C hospitalized at the Musashino Red Cross Hospital, 74 patients of HCV genotype 1b with a high viral load (>100,000 IU/mL by Amplicor-HCV Monitor Assay; Roche Molecular Diagnostics Co, Tokyo, Japan) were included in the present study (Table 1). Patients with cirrhosis, autoimmune hepatitis, or alcoholic liver injury were excluded. No patient was positive for hepatitis B virus–associated antigen/antibody or anti–human immunodeficiency virus antibody. No patient received immunomodulatory therapy prior to the enrollment. Written informed consent was obtained from all the patients, and this study was approved by the Ethical Committee of Musashino Red Cross Hospital in accordance with the Helsinki Declaration. Five patients with nonviral liver disease (2 had autoimmune hepatitis and 3 had primary biliary cirrhosis) were included in the present study as controls.

### *Treatment Protocol*

The patients were treated for 48 weeks with subcutaneous injections of PEG-IFN-$\alpha$-2b (PegIntron; Schering-Plough Corporation, Kenilworth, NJ) at a dose of 1.5 $\mu g \cdot kg^{-1} \cdot week^{-1}$. Ribavirin (Rebetol; Schering-Plough Corporation) was administered concomitantly over the 48-week period, given orally twice daily at a total daily dose of 600 mg for the patients who weighed less than 60 kg and 800 mg for the patients who weighed between 60 and 80 kg. The dose of PEG-IFN-$\alpha$-2b was reduced to 0.75 $\mu g \cdot kg^{-1} \cdot week^{-1}$ when either the neutrophil count was $<750/mm^3$ or the platelet count was $<80 \times 10^3/mm^3$. The dose of ribavirin was reduced to 600 mg/day when the hemoglobin concentration decreased to <10 g/dL.

### *Measurement of Gene Expression in the Liver*

Liver biopsy was performed immediately before starting the therapy. After extraction of total RNA from liver biopsy specimens, the messenger RNA (mRNA) expression of positive and negative cytoplasmic viral sensors (RIG-I, MDA5, and LGP2), the adaptor molecule (Cardif), related ubiquitin E3-ligase (RNF125), and the modulators of these molecules (ISG15 and USP18) was quantified by real-time quantitative polymerase chain reaction (PCR) using primers specific for target genes. In brief, total RNA was extracted by the acid-guanidinium-phenol-chloroform method using Isogen (Nippon Gene Co Ltd, Toyama, Japan) from the liver biopsy specimen, which was 0.2–0.4 cm in length and 13 gauge in diameter. Complementary DNA (cDNA) was transcribed from 2 $\mu$g total RNA template in a 140-$\mu$L reaction mixture using a SYBR RT-PCR Kit (Takara Bio Co Ltd, Otsu, Japan) with random hexamer. Real-time quantitative PCR was performed using Smart Cycler version II (Takara Bio Co Ltd) with the SYBR RT-PCR Kit (Takara Bio Co Ltd) according to the manufacturer's instructions, and intercalating SYBR Green I (Molecular Probes Inc, Eugene, Oregon) was detected. Assays were performed in duplicate, and the expression levels of target genes were normalized to expression of the glyceraldehyde-3-phosphate dehydrogenase (G3PDH) gene and hydroxymethylbilane synthase, which is stable in the liver, as quantified using real-time quantitative PCR as internal controls. For accurate normalization, a set of 2 housekeeping genes was used in the present study. Sequences of primer sets were as follows: RIG-I: 5′-AAAGCATGCATGGTGTTCCAGA-3′, 5′-TCATTCGTGCATGCTCACTGATAA-3′; MDA5: 5′-ACATAACAGCAACATGGGCAGTG-3′, 5′-TTTGGTAAGGCCTGAGCTGGAG-3′; LGP2: 5′-ACAGCCTTGCAAACAGTACAACCTC-3′, 5′-GTCCCAAATTTCCGGCTCAAC-3′; Cardif: 5′-GGTGCCATCCAAAGTGCCTACTA-3′, 5′-CAGCACGCCAGGCTTACTCA-3′; RNF125: 5′-AGGGCACATATTCGGACTTGTCA-3′, 5′-CGGGTATTAAACGGCAAAGTGG-3′; ISG15: 5′-AGCGAACTCATCTTTGCCAGTACA-3′, 5′-CAGCTCTGACACCGACATGGA-3′; USP18: 5′-TGGTTCTGCTTCAATGACTCCAATA-3′, 5′-TTTGGGCATTTCCATTAGCACTC-3′; GAPDH: 5′-GCACCGTCAAGGCTGAGAAC-3′, 5′-TGGTGGTGAAGACGCCAGT-3′. hydroxymethylbilane synthase: 5′-AAGCGGAGCCATGTCTGGTAAC-3′, 5′-GTACCCACGCGAATCACTCTCA-3′.

### *Sequential Measurement of Gene Expression in Peripheral Blood Mononuclear Cells Before and During Therapy*

To understand transcriptional response of the genes to PEG-IFN-$\alpha$-2b and ribavirin therapy, serial expression of RIG-I, RNF125, Cardif, ISG15, and USP18 were determined before and during treatment in peripheral blood mononuclear cells (PBMC) in 14 patients (7 were sustained viral responders [SVR] and 7 were NVR). PBMC was obtained from whole blood samples collected before and at 4, 8, 24, 48, and 168 hours after the initiation of PEG-IFN-$\alpha$-2b and ribavirin combination therapy. After extraction of total RNA from the PBMC, the expression of mRNA was quantified at each specified time point using real-time quantitative PCR as described above. Gene expression levels at each time point during treatment were calculated relative to baseline expression levels measured prior to IFN treatment.

### *Western Blotting*

Western blotting was carried out in 9 patients (5 were SVR and 4 were NVR) and 3 non-HCV control subjects as described previously.[21] Liver biopsy specimen of ~10 mg was homogenized in 100 $\mu$L Complete Lysis-M (Roche Applied Science, Penzberg, Germany). Twenty micrograms of the homogenates were separated by SDS-PAGE and blotted onto a polyvinylidene difluoride Western blotting membrane. The membrane was incubated with the primary antibodies followed by a peroxidase-labeled anti-IgG antibody and visualized by chemiluminescence using the ECL Western blotting Analysis System (Amersham Biosciences, Buckinghamshire, United Kingdom). The anti-VISA mouse monoclonal antibody (BioDesign, Saco, ME) and anti-$\beta$-actin antibody (Sigma Chemical Co, St. Louis, MO) were used.

### *HCV Dynamics in Serum*

To analyze the viral dynamics, HCV RNA was quantified just before and at 4, 8, and 24 hours and 2, 7, 14, 28, 56, and 84 days after the initiation of PEG-IFN-$\alpha$-2b and ribavirin combination therapy, using real-time detection PCR, as reported previously.[22] For each patient, the viral decline curve was plotted on a semilogarithmic scale, and the slopes of the exponential viral declines were calculated for each viral decline phase with a straight-line fit of the data.

### *Definitions of Response to Therapy*

A patient negative for serum HCV RNA during the first 6 months after the completion of PEG-IFN-$\alpha$-2b and ribavirin combination therapy was defined as an SVR, and a patient for whom HCV RNA became negative at the end of therapy and reappeared after completion of therapy was defined as a transient responder (TR). A patient who was positive for HCV RNA even during the course of therapy was defined as an NVR. HCV RNA was determined with the Amplicor qualitative assay (Roche Molecular Diagnostics Co, Tokyo, Japan). The detection sensitivity of this assay is approximately 50 IU/mL.

### *Statistical Analysis*

Categorical data were compared by the $\chi^2$ test and Fisher exact test. Distributions of continuous variables were analyzed by Mann–Whitney $U$ test for 2 groups. Kruskal–Wallis test was used for multiple group comparisons. All tests of significance were 2-tailed, and $P$ values $< .05$ were considered statistically significant.